CONTROLLING THE FEEDRATE OF MATERIAL FROM A VIBRATORY PIPE CONVEYOR USING AN ELECTRO-MAGNETIC VIBRATOR AND LOAD CELL SYSTEM

SUBMITTED IN COMPLIANCE WITH THE

REQUIREMENTS FOR THE NATIONAL MASTER'S DIPLOMA IN

TECHNOLOGY IN THE DEPARTMENT OF ELECTRONIC ENGINEERING

AT TECHNIKON NATAL

GARY PETER JANSE VAN VUUREN

MARCH 1994

I hereby declare that this dissertation represents my own work both in conception

Approved for final submission

Professor E Eitelberg
Supervisor

SUPERVISOR'S : Professor A B Stewart Ph.D.(UCT)

Assistant Director, Measurement and Control Division,

Council for Mineral Technology

(July 1986 to July 1987)

Professor E Eitelberg Dr.-Ing. habil

Department of Electrical and Control Engineering

University of Durban-Westville

(March 1988 to June 1993)

Acknowledgements

For the many hours of patient explanations and suggestions I wish to thank my second supervisor, Professor Eitelberg, without whose assistance this work would not have been possible. My thanks also to Professor Stewart, now living in Australia, Mr Gunter Sommer and to Mintek. They introduced me to this topic, over which I have spent many hours, sometimes frustrating, but always learning.

I wish to thank the many people at Technikon Natal for their advice, assistance, argument and encouragement. There are many of you and the time you gave me has been most appreciated. In particular I would like to thank Mr Tony Allinson and Mr Bruce Galbraith for their assistance in writing the software.

The Foundation for Research Development of the CSIR and the Department of Research Development at Technikon Natal are gratefully acknowledged for their financial assistance.

Abstract

This work presents a novel way of controlling the feedrate of raw material from a vibratory pipe feeder system. The system consists of a hopper, feeder pipe, electromechanical vibrator and a loadcell which measures the mass of the complete system. Raw material is gravity fed onto the vibrating pipe whose amplitude of vibration controls the amount of material fed.

Because of the mechanical design of the system a considerable degree of non-linearity in terms of the gain exists. This non-linearity occurs mainly because the force due to the mass of raw material in the hopper acts directly on the feeder pipe. Therefore, when the hopper is full considerable damping of the vibration exists and as the hopper empties so this damping decreases. Furthermore the change in mass relative to the total mass is small and this leads to high noise levels and the attendant difficulty in obtaining a meaningful and accurate mass signal.

Filtering, both analog and digital, is done and by taring out the fixed masses (hopper, pipe, electromechanical vibrator, stand etc) from the loadcell signal a measure of the mass of raw material remaining in the system is obtained. By differentiating this signal with respect to time a signal representative of the feedrate of raw material is achieved.

The feeder system is then modelled as a plant with a variable gain and integrator only. After investigation of the way in which the gain varies a computer algorithm is used to implement gain scheduling according to the mass of raw material remaining in the hopper. In this way the amount of the variation in the magnitude of the plant gain is reduced to an acceptable level for control purposes. It is then

Uittreksel

Hierdie verhandeling beskryf 'n buitengewone metode om die voertempo van 'n grondstof uit 'n vibreerpypvoerder te beheer. Die stelsel bestaan uit 'n voerbak, voerpyp, elektromeganiese vibrator en 'n lasmeter om die massa van die hele stelsel te bepaal. Die grondstowwe word met valtoevoer in die vibrerende voerpyp gestort. Die amplitude van vibrasie daarvan beheer die toevoertempo.

As gevolg van die ontwerp is daar 'n redelike hoë mate van nie-liniariteit in die stelsel teenwoordig. Hierdie nie-liniariteit is in hoofsaak te wyte aan die feit dat die massa van die grondstof in die voerbak 'n krag direk op die voerpyp uitoefen. Demping van die voerpyp se vibrasie is dus maksimum wanneer die bak vol is en neem gelydelik af namate dit leër word. Verder is die verandering van die massa klein relatief tot die totale massa. Dit veroorsaak dat geraas 'n hoë vlak bereik wat dit moeilik vir die bediener maak om'n sinvolle en akkurate massasein te bekom.

Filtrering, analoog sowel as digitaal, word uitgevoer. Deur die massas van die voerbak, voerpyp, elektromeganiese vibrator, onderstel, ensovoorts van die lasmetersein af te trek, word die massa van die oorblywende grondstof in die stelsel bepaal. Deur hierdie sein te differensieer met betrekking tot tyd, word sodoende 'n sein bekom wat die voertempo van die grondstof verteenwoordig.

Die pypvoerder word gemodelleer as 'n toestel met slegs 'n verstelbare wins en integreerder. Nadat vasgestel is hoe die wins varieer, word 'n rekenaaralgoritme gebruik om winsskedulering te implementeer volgens die massa van die oorblywende grondstof in die bak. Hierdeur word die variasie in die grootte van die wins beperk tot 'n aanvaarbare vlak vir beheerdoeleindes. Verder word dan aangetoon dat hierdie

shown that the compensated plant is satisfactorily controlled using a simple integral controller only. The design of the controller is based on the Quantitative Feedback Theory (QFT) (Horowitz 1985) with special emphasis on the usefulness of the inverse Nichols chart.

Finally the effectiveness of the digital filter is examined and the gain scheduling is verified, by comparing the plant performance with and without the gain scheduling. The dissertation concludes by illustrating another common industrial problem where the use of gain scheduling could lead to a far simpler means of control than that of conventional proportional, integral and derivative (PID) control.

gekompenseerde stelsel bevredigend beheer kan word deur slegs van 'n eenvoudige integraalbeheerder gebruik te maak. Die ontwerp van die beheerder is gebaseer op die Kwantitatiewe Terugvoerteorie (Quantitative Feedback Theory, QFT) (Horowitz 1985), met spesiale verwysing nadie bruikbaarheid van die omgekeerde Nicholskaart.

Laastens word die doeltreffendheid van die digitale filter ondersoek en die winsskedulering geverifieer deur die werkverrigting van die stelsel te vergelyk met en sonder die winsskedulering. Ten slotte beskryf die verhandeling 'n verdere algemene industriële probleem waar winsskedulering kan lei tot 'n veel eenvoudiger metode van beheer as die konvensionele proporsionele, integrale en derivate (PID) beheer.

Contents

List of figures

List of tables

Constants and abbreviations

When compiling the following list, the symbols shown reflect those used in the text. Some slight deviations from these and other abbreviations have been used in the software.

Sampling rate	:	1 second	
Mintek	:	Council for Mineral Technology.	
T	:	Arbitrary time interval.	[sec]
m, m(t), M(s)	:	Mass of digital filter input.	[kg]
m_{AVE}, mave, $M_{AVE}(s)$	:	Mass of digital filter output.	[kg]
g_w	:	Frequency dependent gain.	[rad/s]
a_k, $\|a_k\|$	:	Magnitude of fft of filter output.	
K, KK	:	Setpoint feedrate.	[kg/hr, kg/s]
ff	:	Measured feedrate.	[kg/hr]
ee	:	Error feedrate.	[kg/hr]
u, U	:	Controller output.	[kg/s]
Y, Y(s)	:	Output of gain compensator block.	
D, D*	:	Disturbance input.	
ff	:	Measured feedrate.	[kg/hr]
k_{var}, k(m)	:	Mass dependent variable gain.	
G_{MOD}	:	Modified gain compensator gain.	
a, b	:	Constants.	
M(s)	:	Plant output.	
L, L(jw), L(s)	:	Open loop transfer function.	
G, G(s)	:	Controller transfer function.	
P	:	Plant transfer function.	
F	:	Filter transfer function.	

Chapter one

THE PROBLEM AND ITS SETTING

1.1 INTRODUCTION

The accurate control of the feed rate of the raw materials into a plasma arc furnace forms the basis of this investigation.

Electricity, as a source of heat energy for steel making, had its beginning in 1878 when William Siemens designed the first electric furnace (South African Iron and Steel Corporation 1953). It was another 22 years before a French mining engineer, Dr Paul Heroult, built an electric arc furnace (van Thoor 1970).

Since then several ways of electrically heating furnaces have been used. According to the Encyclopedia of Chemical Engineering (1980), these can be grouped into three categories each with sub-categories :

1. electric resistance furnaces,
2. electric arc furnaces and
3. electric induction furnaces.

Plasma arc furnaces fall in the second category and have received intensive evaluation for the production of ferro-alloys in a number of countries in recent years (Barcza and Stewart 1983). South Africa is no exception and the Council for Mineral Technology (Mintek) has been at the forefront of these investigations (Barcza and Stewart 1983). According to Barcza and Stewart (1983), "Mintek aims at bridging the gap between important small-scale fundamental research into plasma

and actual industrial pyrometallurgical applications".

The potential advantages of plasma arc technology have been variously documented (Barcza and Stewart 1983, Nicol *et al.* 1986), but some are of importance here :

1. In the case of Mintek, being a research institute, any facility would be required to have as much flexibility as possible and a d.c. plasma arc furnace allows for this flexibility.

2. The lack of the need for careful sizing of raw materials as required in the more common submerged arc furnace. In other words, the plasma furnace will operate with raw materials of varying particle sizes.

3. The ability to use widely varying levels of operating power and to vary the feed rate of the different raw materials independently of each other, to produce a specific ferro-alloy.

The South African ferro-alloy industry and Mintek are co-operating towards the realization of full scale production of high carbon ferrochromium. In 1980 Mintek decided to install a d.c. plasma pilot plant and this has over several years grown from a small 100kVA facility to a large scale 3.2MVA plant capable of sustained power levels greater than 1MW (Nicol *et al.* 1986). Mintek's research objectives are clearly defined as presented in the paper by Barcza and Stewart (1983).

The conclusions Mintek has come to with regard to the control and operation of their plasma arc facility (Nicol *et al.*1986) are:

1. That the d.c. plasma arc furnace can be used to replace the conventional submerged arc furnace for the production of ferro-alloys.

2. That consistent stable metallurgical performance can be achieved provided an adequate level of control over the operation is exercised.

3. That the most important control functions are the accurate control over the feed rate of raw materials, the accurate control of the input electrical power and the setting of the ratio of the feed of raw materials to the electrical power.

A complete discussion of the operation of the plasma arc furnace at Mintek can be found in the paper by Nicol *et al.* (1986).

The feed system developed by Mintek consists of three hoppers, to avoid segregation of the feed, supplying raw material via vibrating pipe feeders, see Fig 1. Each pipe feeder is controlled by an electro-magnetic vibrator actuator, where the feed rate is dependent on the amplitude of vibration. A loadcell measures the mass of the hopper and feeder pipe, including the raw material.

The control system used, forces the loadcell signal (mass of the raw material) to follow, in time, a signal of the form of a linear ramp (Nicol *et al.* 1986), thereby emptying the hopper at a constant rate.

A major problem, identified by Mintek (Stewart 1986a), relates to the dead time at start up, that is, the time required to fill the pipe before any material is actually fed. A further problem is that of the change in feed rate without a demand for this change (Stewart 1986a). This is because the magnitude of vibration of the feeder pipe is

damped by the raw material resting on it and as the hopper empties, this damping decreases, even for the same input signal, and the feed rate increases. In addition, Mintek felt, that a better understanding of the dynamics of the feed system would be of major importance to the overall understanding, and thus for the proper control design to improve the operation and performance of the plasma furnace (Stewart 1986b).

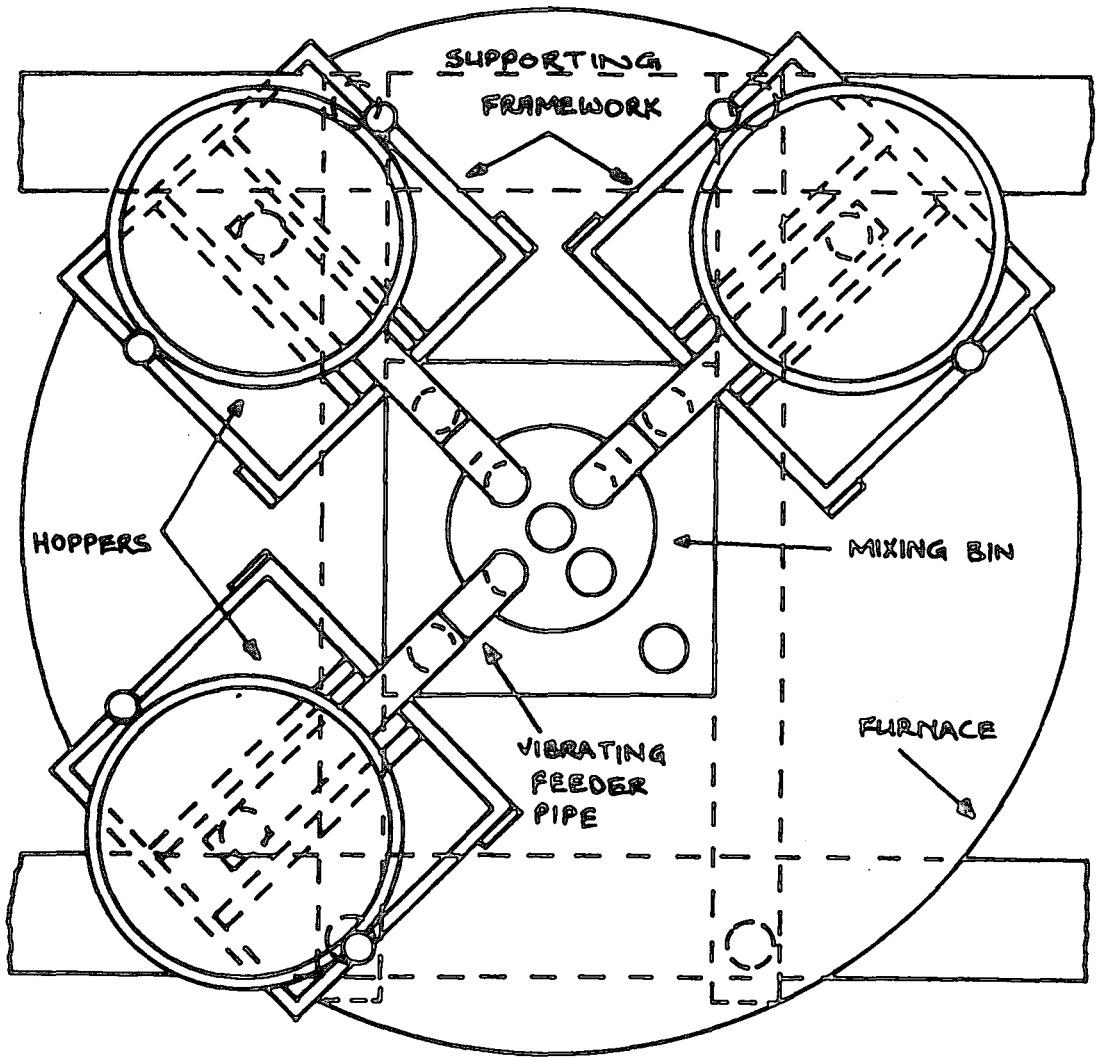

Fig 1. Plan view of three hopper system developed by Mintek.

The dead time problem is a physical consequence of the plant and its reduction cannot be influenced. However, the second problem, that of the change in feed rate without there being a demand for it, is to be investigated in this study.

The way in which the feed rate of the plant varies can be considered as a change in plant gain and a means of reducing the amount of uncertainty in this plant gain will be implemented. Thereafter a controller will be designed to force the closed loop response of the plant to be acceptable. This is the approach adopted in this study.

As will be seen later, a crucial component of the design method to be used is "gain scheduling". It is assumed throughout this report that the method of "gain scheduling" is applicable. An important potential advantage of this form of control is the wider applicability in similar classes of control problems.

1.2. THE SUBPROBLEMS

The analysis of the overall problem, namely of achieving an actual feed rate equal to that of the required feed rate under all hopper "fullness" situations, shows that it is possible to distinguish several separate subproblems.

1.2.1. MECHANICAL OPTIMIZATION

The first phase of the project involves assembling the mechanical parts, that is, to construct the hopper feeder system. The design allows for the adjustment of two variables, firstly the size of the feed aperture and secondly the relative position of the hopper to the feeder pipe. This second variable allows the hopper outlet to be moved along the length of the feeder pipe, obviously within certain limits. The "optimum" (see Chapter 2) positions for these two variables has to be found.

1.2.2. DESIGN OF THE CONTROL SYSTEM

After examination of the dynamics of the plant it is proposed to design and implement a digital control strategy. The controller is required to force the actual feed rate to follow the required feed rate under all hopper "fullness" situations.

1.3. THE DELIMITATIONS

Because of the broad scope of this project several delimitations have been made, some of which are purely financially based.

1.3.1. THE HOPPER SYSTEM

Due to financial constraints the plant that was constructed consists of only one hopper and feeder pipe with the associated instrumentation, see Fig 2. The system is exactly the same size as that being used by Mintek. However because only one hopper is to be used it does mean that the ratio mode of operation (Stewart 1986a) cannot be implemented. The ratio mode of operation is a ratio of contributions from each of the three hoppers. The non-implementation of the ratio mode of operation is not considered to be detrimental to the investigations in any way because the control strategy would be the same for each of the three hoppers. The photographs in Fig's 3 and 4 show the construction of the system at Technikon Natal.

1.3.2. THE RAW MATERIAL

The vast majority of raw materials in South Africa, for the production of ferro-alloys, varies quite considerably in consistency, from fine powder to "golf ball" size.

However, dry beach sand with uniform particle size will be used for all experiments. The implication of this is that rapid changes in the measured mass will be avoided (when a large piece of the raw material leaves the feeder pipe). The controller design, being based on the mass of the raw material, is considered robust enough to take care of any inconsistencies in the particle size in the raw material. This is, of course, an idealization of the real experimental situation at Mintek.

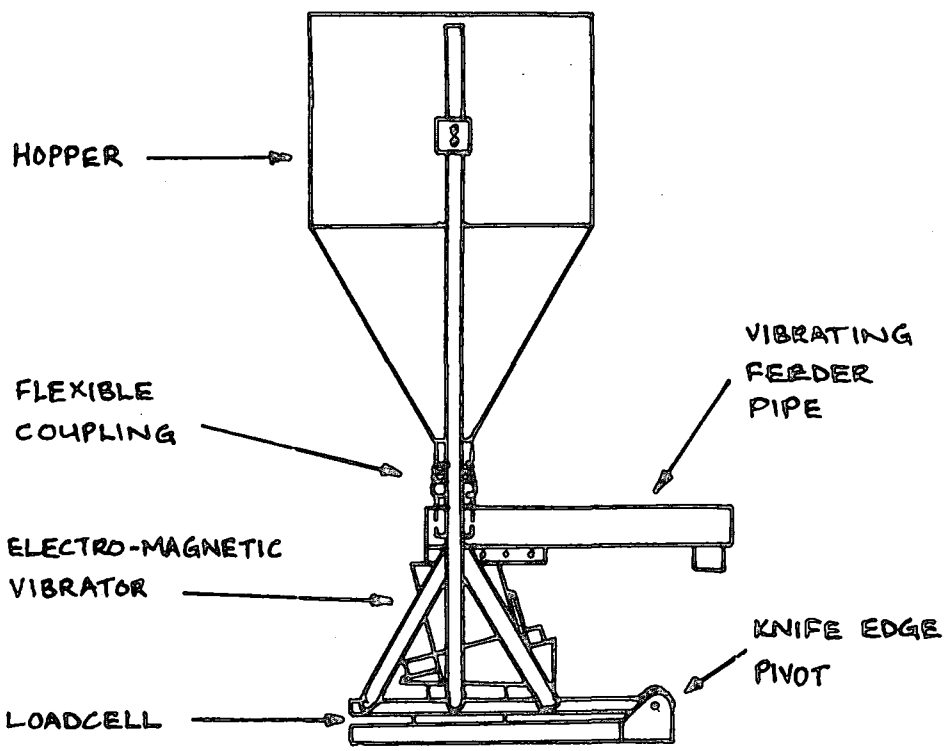

Fig 2. Single hopper system constructed at Technikon Natal.

1.3.3. THE PROBLEM OF NOISE

The environment, at Mintek, in which the feeder system is expected to operate is extremely noisy, both electrically and mechanically. The system physically sits on top of the furnace. At Technikon Natal only one hopper/feeder system, as shown in Fig 2, was built. Because the vibrator actuator is mounted directly on top of the loadcell (mass sensor) the noise due to mechanical vibration is expected to be the

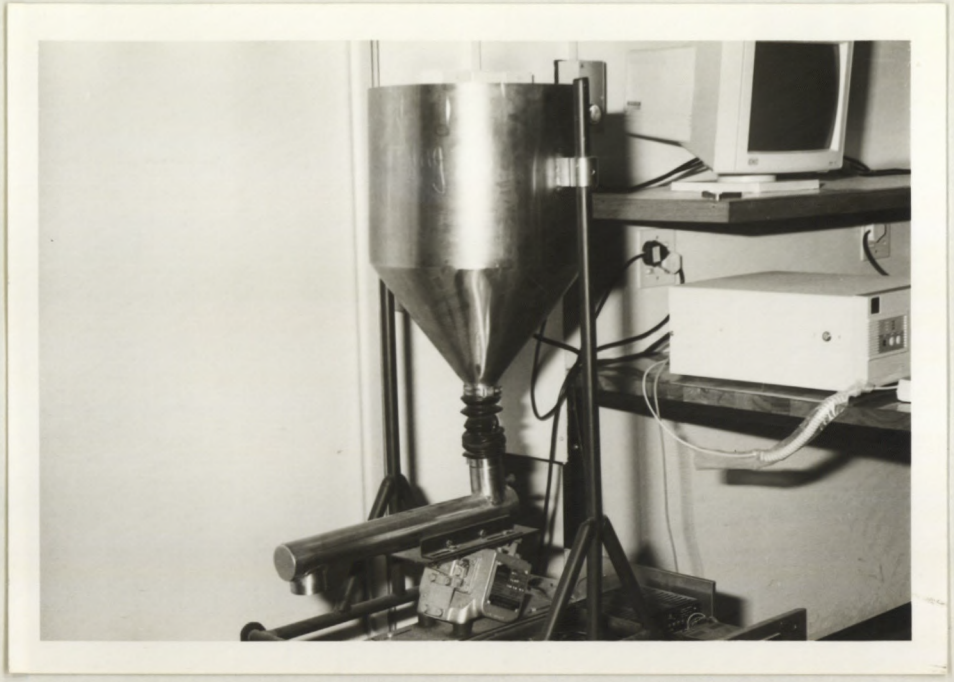

Fig 3. Photograph showing the hopper and feeder pipe.

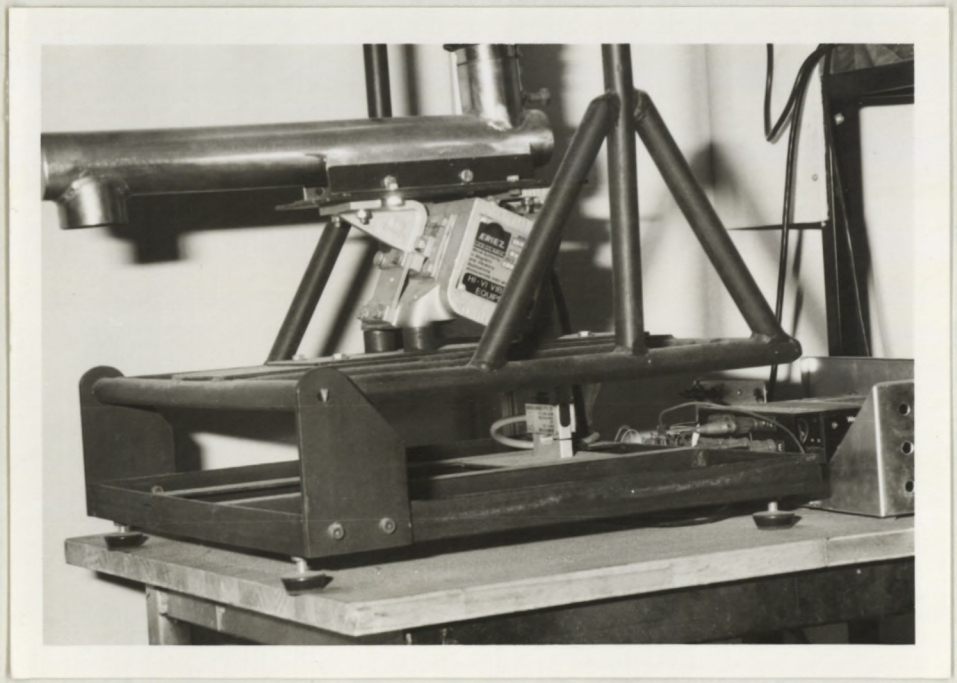

Fig 4. Photograph showing the loadcell arrangement.

dominant noise effect. The project is done under these "laboratory" conditions and no artificial arrangement is made to introduce additional noise.

Chapter two

MECHANICAL OPTIMIZATION

2.1 INTRODUCTION

The feeder system design makes allowance for the variation of two parameters. Firstly, the vibrator actuator can be moved relative to the feeder pipe and secondly the entrance aperture for the raw material into the pipe can be varied, see Fig 5. The first variable has been divided into five possible positions and the second, into three possible positions. Because the financial constraints did not allow the purchase of a PC at this stage and hence allow data to be captured, a record of the mass was obtained by feeding the loadcell amplifier's output directly into a continuous chart recorder. This means that the charts appear backwards, that is, with the hopper full and time equal to zero on the right. The hopper empties towards the left.

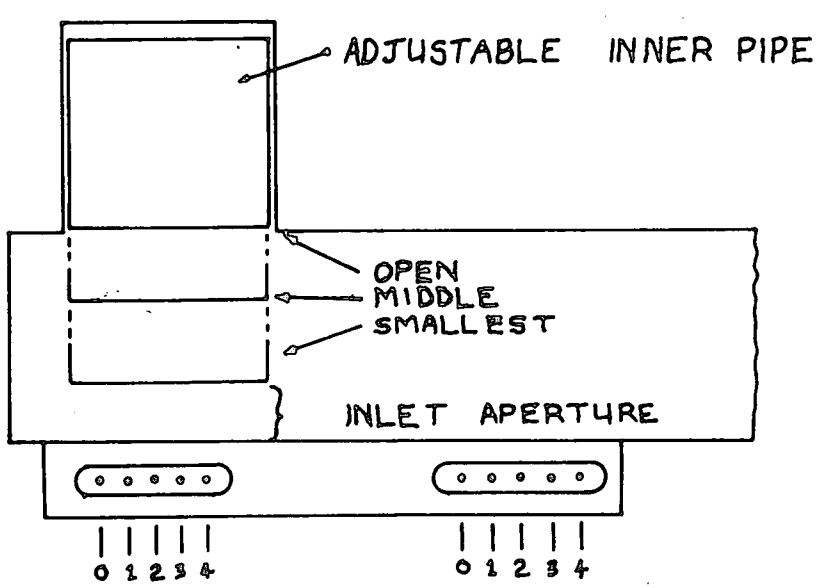

Fig 5. The two mechanical variables.

2.2 OPTIMIZING THE TWO VARIABLES

Early observations, to establish the maximum possible operating voltage at the extremes of the two variables, revealed firstly that the electromagnetic vibrator could not be operated above two hundred volts when the hopper was nearly empty. This is because of "hammering" of the two sides of the magnetic core, within the actuator. Secondly that while emptying, at a certain "fullness", there would be a rapid increase in the feed rate (change in slope). This "fullness" occurred at approximately 22 kg. Fig's 6 to 9 show the responses at the extremes of the two variables where the horizontal axis represents time and the vertical axis the mass.

The first problem was overcome by running all tests at 185 volts. This would ensure that no hammering occurred. To overcome the second problem it was decided, in this mechanical setting up, to look for the most linear feed rate in the mass region from full down to approximately 23 kg. Terminal based linearity (Considine 1974), that is where the upper and lower range values, in this case "full" (approximately 40 kg) and 23 kg, are joined by a straight line and the deviation measured, was used as a means of judging the relative linearities over the range of masses in question. An example of the procedure used is shown in Fig 6.

The actuator position is divided into five one centimetre markings where position 0 is with the actuator furthest from the material outlet and position 4 closest (see Fig 5). The raw material feed aperture has three positions, labelled as :

OPEN	-	largest possible position
MIDDLE	-	slightly smaller opening
SMALLEST	-	smallest possible opening

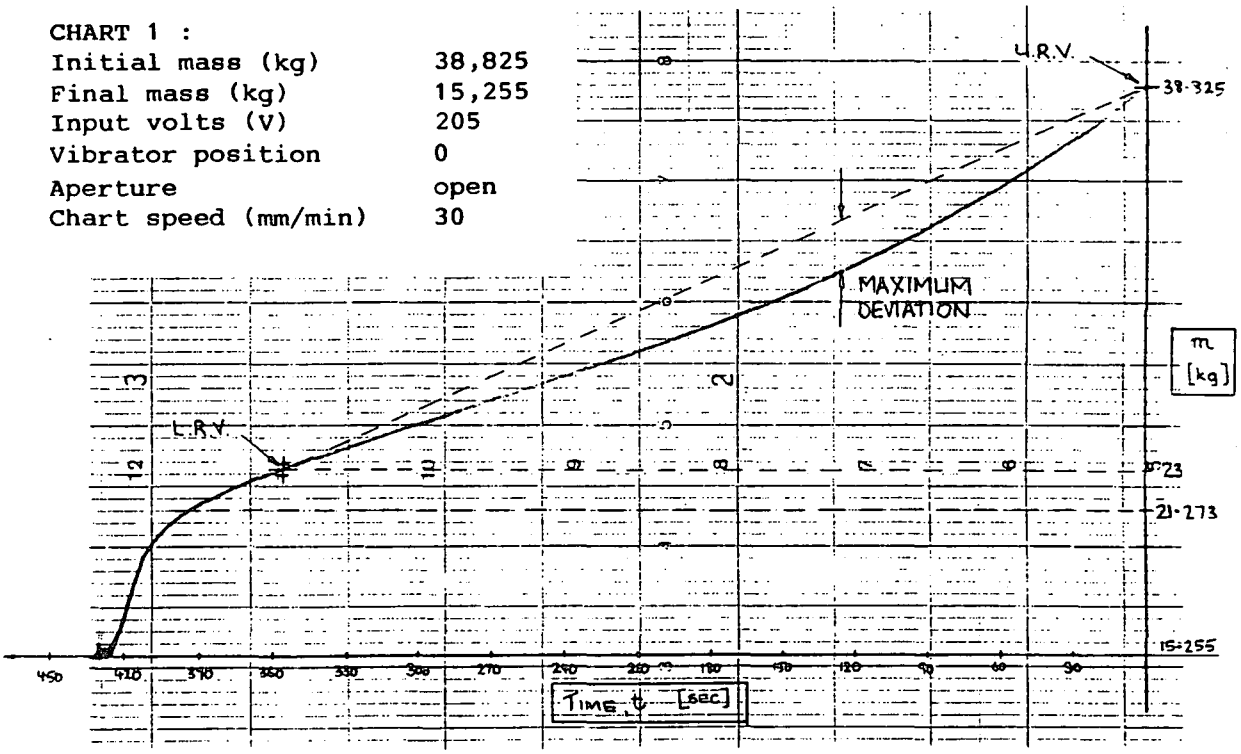

Fig 6. Chart one : actuator 0, aperture open.

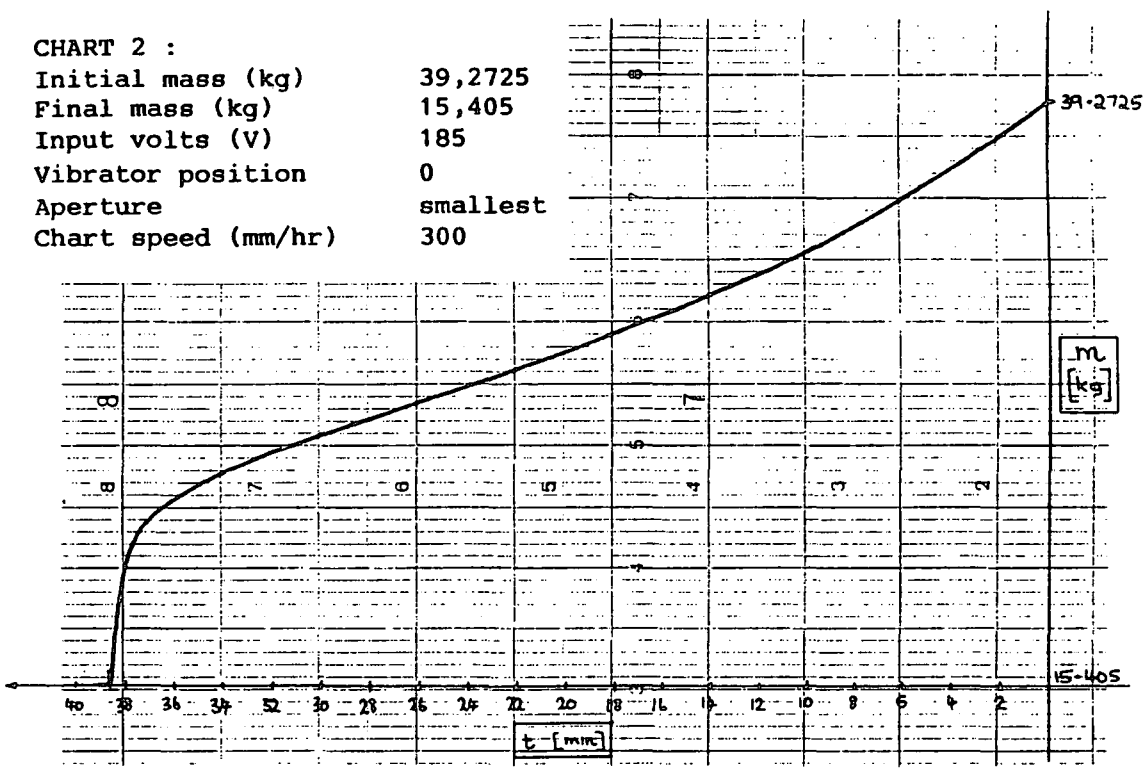

Fig 7. Chart two : actuator 0, aperture smallest.

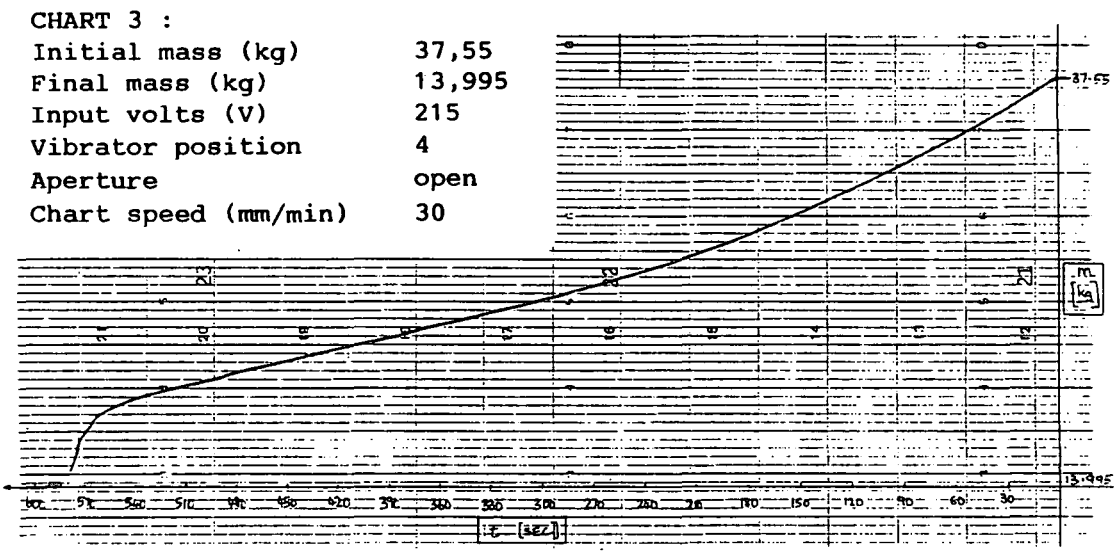

Fig 8. Chart three : actuator 4, aperture open.

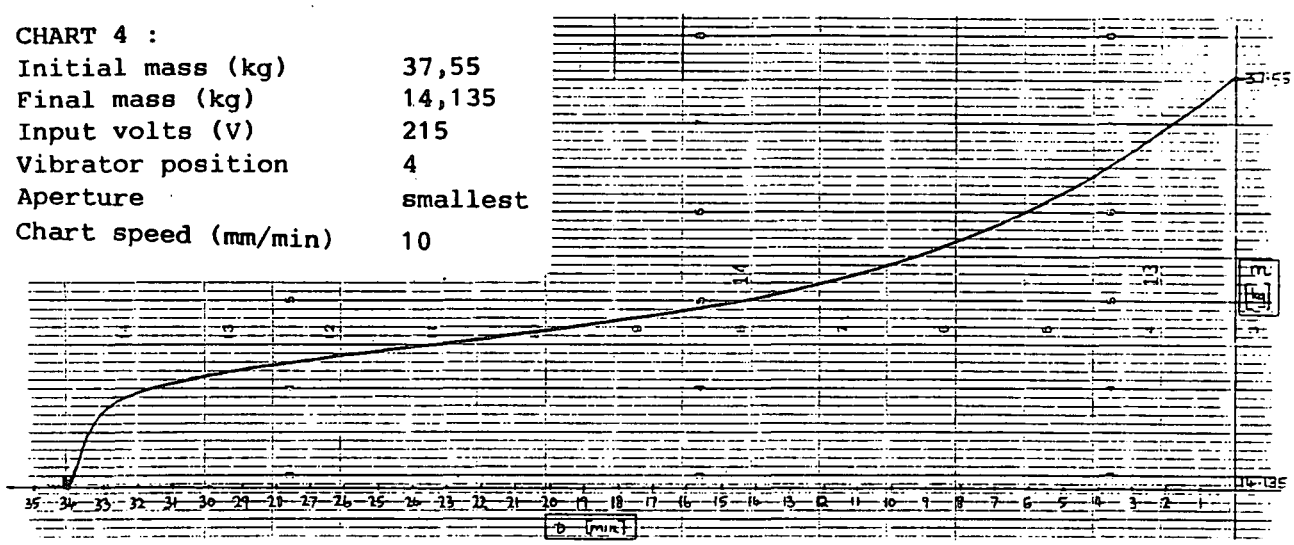

Fig 9. Chart four : actuator 4, aperture smallest.

Fifteen test runs were done covering all possible combinations of the two variables, and these charts are shown in Appendix A. A summary of the percentage deviations is shown in Table 1 where test run number eight is chosen as the most linear.

CHART #	5	6	7	8	9	10	11	12
ACT. POS.	0	0	0	1	1	1	2	2
FEED APERT.	OPEN	MID	SMALL	OPEN	MID	SMALL	OPEN	MID
U.R.V. [kg]	40.275	40.275	40.225	39.650	40.025	39.975	39.600	39.750
L.R.V. [kg]	22.950	22.900	22.875	22.975	22.975	22.900	22.950	22.925
DEVIATION [kg]	1.551	1.965	1.859	1.132	1.658	3.312	1.953	3.488
DEVIATION [%]	8.95	11.310	10.710	6.790	9.700	19.390	11.730	20.730

CHART #	13	14	15	16	17	18	19
ACT. POS.	2	3	3	3	4	4	4
FEED APERT.	SMALL	OPEN	MID	SMALL	OPEN	MID	SMALL
U.R.V. [kg]	39.650	39.275	39.150	39.150	38.975	38.625	38.775
L.R.V. [kg]	22.925	22.875	22.925	22.925	22.975	22.975	22.900
DEVIATION [kg]	3.717	2.475	3.594	3.626	2.487	2.986	3.599
DEVIATION [%]	22.220	15.090	22.150	22.350	15.540	19.080	22.670

Where : U.R.V. = upper range value; L.R.V. = lower range value.

Table 1. Percentage deviations for all combinations of the two mechanical variables.

2.3 CONCLUSIONS

With the experiments done and presented in this part of the project a good feel for the plant behaviour can be obtained. Important knowledge of the way in which the feed rate of the plant suddenly increased at a certain fullness may be gained at this stage. The experimental method of optimization is very rough. Chart number 8 has the smallest percentage deviation and therefore its settings were chosen for the duration of this project.

Chapter three

SYSTEM DESCRIPTION AND CONFIGURATION

3.1 INTRODUCTION

With the physical plant variables fixed in their two positions the next phase of the project entailed the purchasing and installation of a PC and peripherals, to enable data acquisition and control. This chapter deals with the hardware components as well as the filter implemented in software and concludes with a complete block diagram of the system, where essentially only three blocks, namely the "plant", "controller" and the "gain compensator", remain to be identified.

3.2 DESCRIPTION AND CONFIGURATION

Fig 2 shows the system constructed at Technikon Natal. An electro-magnetic vibrator driven by a phase controller circuit (supplied by Mintek) provides the driving force to the conveyor. The input to the phase controller is 0 to 10 volts. The hopper and stand are mounted on knife edge hinges on one side with a single loadcell forming the other support. A loadcell amplifier forms a part of the output circuit and gives a voltage signal indicating the weight of the raw material in the hopper, as well as the weight of the hopper and stand. The weight of the hopper and stand is later tared out in software.

The loadcell amplifier output was monitored for noise, and an unacceptably high mains (50 Hz) induced component was initially detected. A second order, unity gain, active low pass Butterworth filter (Jay 1988), with a corner frequency of 3 Hz, was implemented. This would reduce the mains component of the noise by more

than 40 dB. The filter circuit is shown in Fig 10.

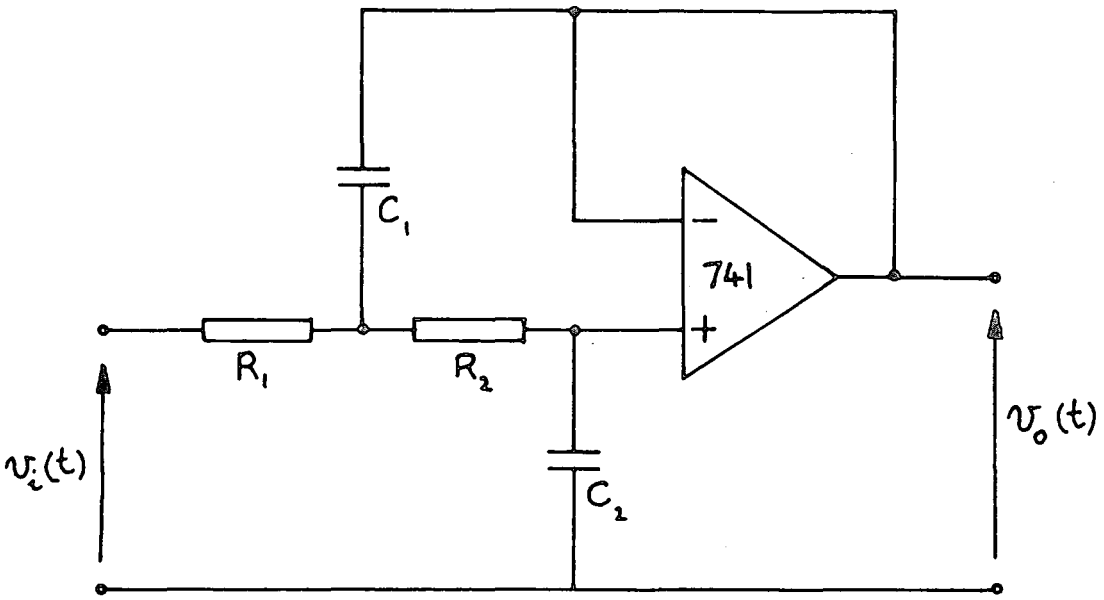

Fig 10. Circuit diagram of analog filter.

The calculation of the circuit parameter values is done according to normalized values (Jay 1988). This approach allows the designer flexibility in the choice of the components. For this filter the normalized values are:

$$R_1' = R_2' = 1\ \Omega$$

$$C_1' = 1.414$$

$$C_2' = 0.7071$$

Denormalizing, or scaling, is done according to the following equations:

$$R_{1,2} = R_{1,2}' * R_x$$

$$C_{1,2} = \frac{C_{1,2}'}{R_x * w_x}$$

where R_x and w_x are values chosen by the designer.

With the corner frequency already chosen to be 3 Hz and choosing R_x to be 150 kΩ the capacitor values are calculated to be:

$$C_1 = 500\ nF$$

$$C_2 = 250\ nF$$

Choosing the preferred values of C_1 = 470 nF and C_2 = 250 nF a corner frequency of slightly more than 3 Hz results. As this is a unity gain filter with negligible phase shift at the system working frequencies (typically less than 1 Hz), the transfer function of the filter can be considered to be approximately unity at the working frequencies.

With the computer and data acquisition hardware available the output of this analog filter was used as the input to the computer. The approach to be taken would require the mass signal to be differentiated, in order to obtain a feed rate signal. Differentiation of a noisy signal is known to be a sensitive and inaccurate operation. Even after the initial filtering it was found that the noise component of this mass signal was still unacceptably high and would require further filtering. It was decided that this additional filtering would be done in software.

Because of having successfully used a moving average filter on a practical installation, this type of filter was selected. This would ensure only two calculations, namely, one of addition and one of division, to generate each data point. The number of points averaged would determine the smoothness of the filter output, where more points would give a better noise reduction but would increase the calculation time taken and decrease the filter bandwidth. After some experiments with the number of sampling points it was decided to use the average of 50 points.

In order to derive the transfer function of this filter, the effects of sampling, introduced by the analog to digital converter, are neglected. Fig 11 shows the input, m(t), to the filter where the output is $m_{AVE}(t)$.

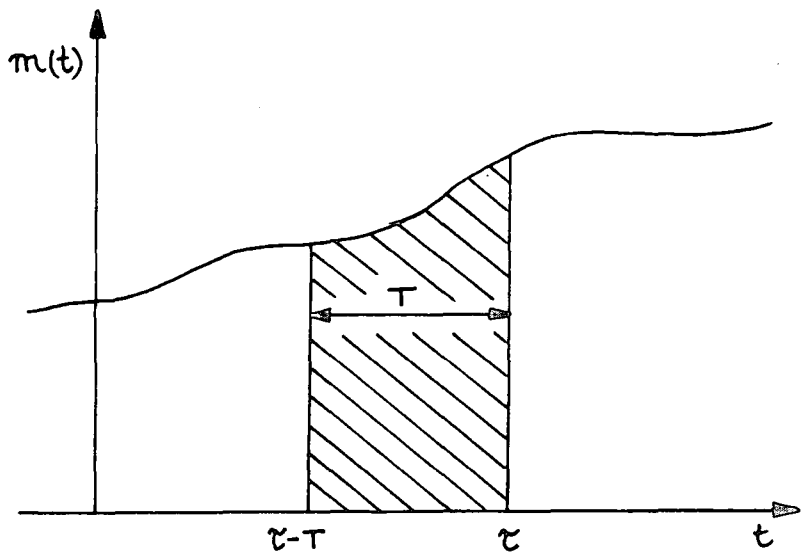

Fig 11. Diagram showing input to digital filter.

The derivation is as follows:

$$m_{AVE}(t) = \frac{1}{T} * \int_{t-T}^{t} m(\tau)\, d\tau$$

$$= \frac{1}{T} * \left[\int_{-\infty}^{t} m(\tau)\, d\tau - \int_{-\infty}^{t-T} m(\tau)\, d\tau \right]$$

now let : $$y(t) = \int_{-\infty}^{t} m(\tau)\, d\tau$$

$$\therefore \quad y(t-T) = \int_{-\infty}^{t-T} m(\tau)\, d\tau$$

so that : $$m_{AVE}(t) = \frac{1}{T} * [\, y(t) - y(t-T) \,]$$

Now taking Laplace transforms of the time signals y(t) and $m_{AVE}(t)$ one gets:

$$Y(s) = \frac{1}{s} * M(s)$$

also

$$M_{AVE}(s) = \frac{1}{T}\left[Y(s) - Y(s) * e^{-T*s}\right]$$

$$= \left[\frac{1 - e^{-T*s}}{T}\right] * Y(s)$$

$$\therefore \quad M_{AVE}(s) = \left[\frac{1 - e^{-T*s}}{T*s}\right] * M(s)$$

The delay time, T, in the above transfer function is easily established by considering the software listing on page 65. The analog to digital converter samples every one tenth of a second (set by the value of "stddelay") with the average taken over fifty samples (set by the value of "wlen"). This means that there are forty nine time delays, each of one tenth of a second duration, giving the value of T to be 4.9 seconds.

It should however be noted that it is only every tenth value (set by the value of uptime) that is used to generate an output from the computer, that is, to control the plant. This means that the loop update frequency is one Hertz.

In order to verify the effectiveness of the filter, firstly a Bode magnitude plot was drawn and is shown in Fig 12. Although the filter is of fiftieth order, because fifty points are averaged, the cut-off characteristic has a slope of -20 dB/dec. The sharp attenuation dips are caused by the dead time, T, where the frequencies at which they occur are the values of the zeroes of the filter transfer function. The first one, for example, being at the frequency w = 1.282 rad/s. The corner frequency is 0.6 rad/s.

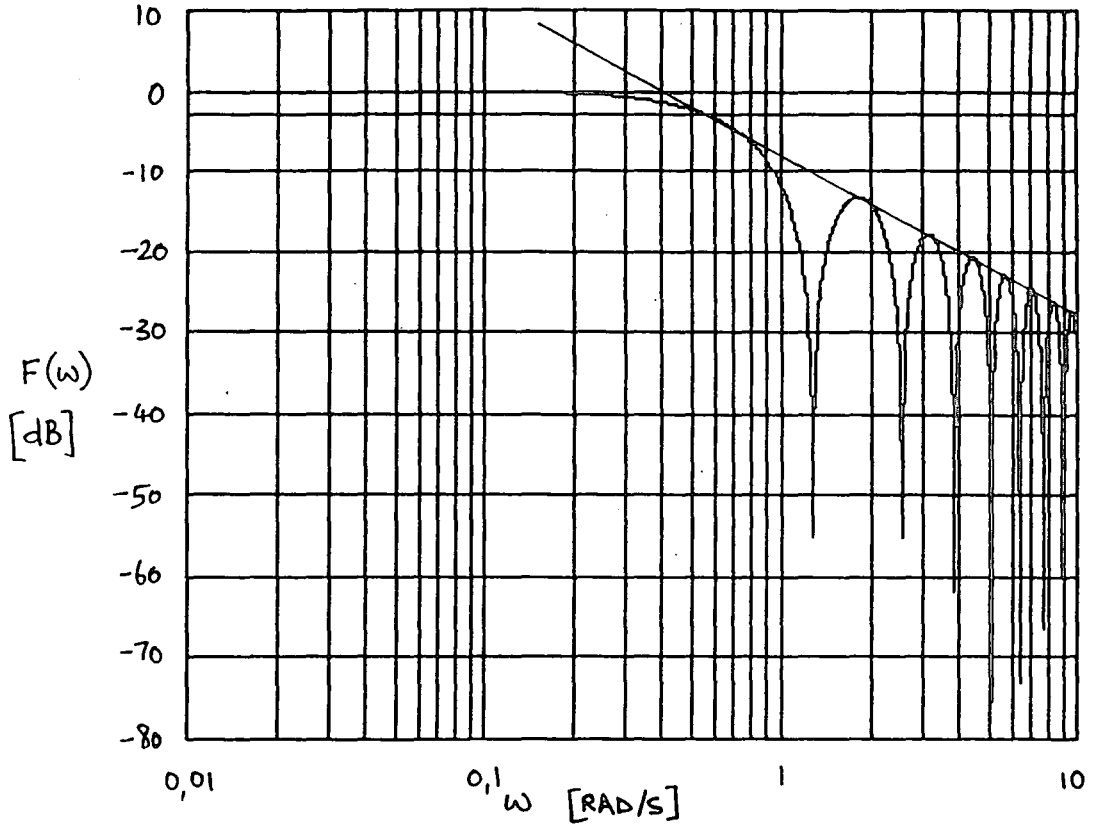

Fig 12. Bode magnitude plot of the filter transfer function.

Secondly a test run was done at the maximum feedrate and the mass values at the filter input and output were recorded. A Fourier transform was then done on each to obtain the frequency response. Plots of the magnitude of this frequency response at the filter input and output are shown in Fig's 13 and 14. The effect of the filter is quite obvious and the zeros of the Bode plot can again be seen in Fig 14. The frequency axis of the Bode plot is logarithmic, while that of the two Fourier transform plots is linear.

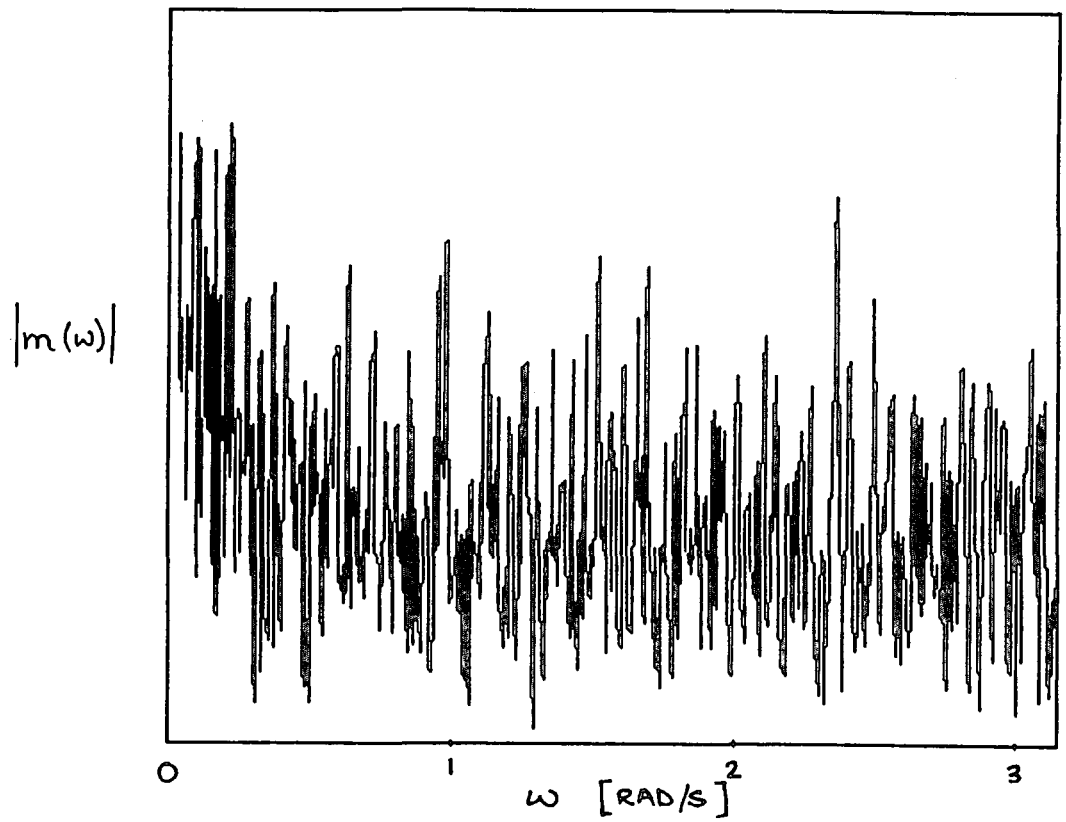

Fig 13. Fourier transform of data before filter.

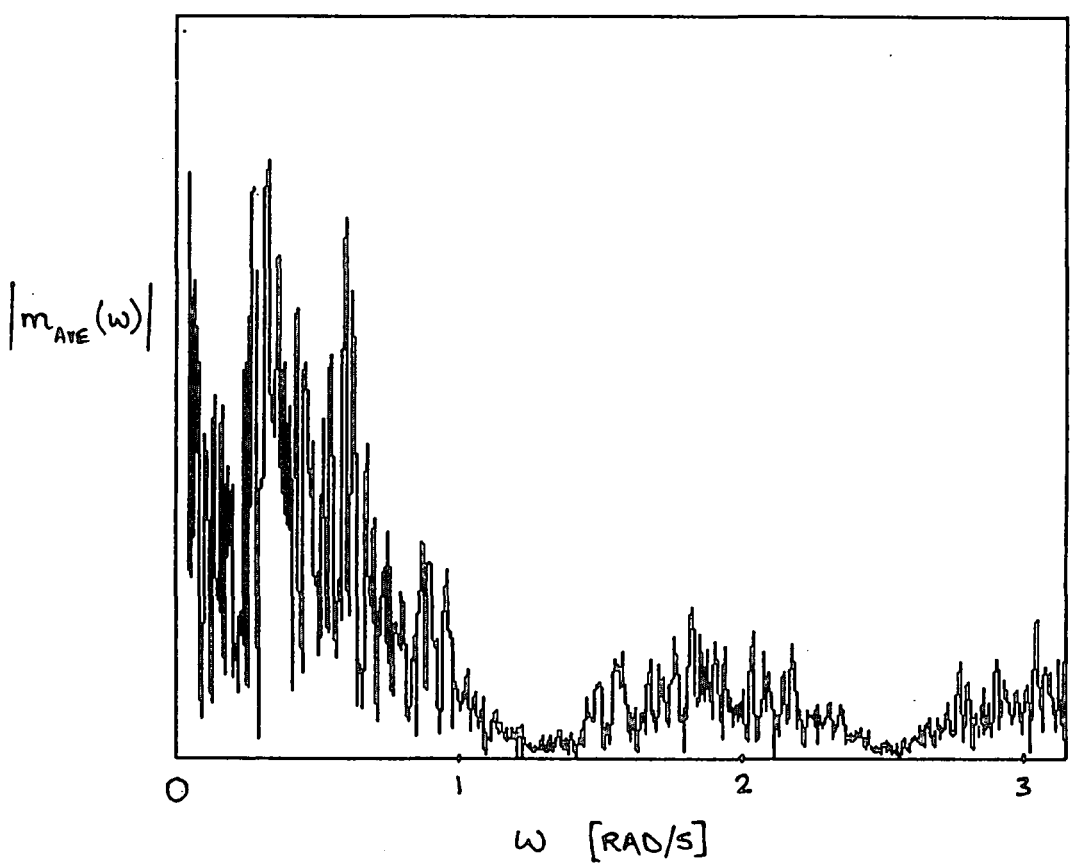

Fig 14. Fourier transform of data after filter.

3.3 BLOCK DIAGRAM OF THE COMPLETE SYSTEM

The block diagram of Fig 15 shows the complete system as finally constructed. The symbols used in this diagram are the same as those used in the software program (see Appendix B for the software listing). The differentiator is used to convert the mass signal into a feed rate signal. The disturbance input, D, is placed somewhat arbitrarily after the plant. It represents all sources of noise, the 50 Hz mains component, noise due to the mechanical vibration, sensor noise, etc.

3.4 CONCLUSIONS

The derivations performed so far establish the transfer functions of all but three of the blocks shown in Fig 15, namely the "plant", "controller" and the "gain compensator". These three will be derived in the following chapters.

The use of both analog and software filtering was not planned but rather evolved as the project developed. Initially it was thought that an analog filter would be sufficient. However, once the software filter had been implemented, the advantages in the use of digital filtering became obvious. The lack of the need for a separate power supply (a passive discrete component filter could have been used), the versatility in the use of software and the continued noise problems with hardware filtering can be considered the most important.

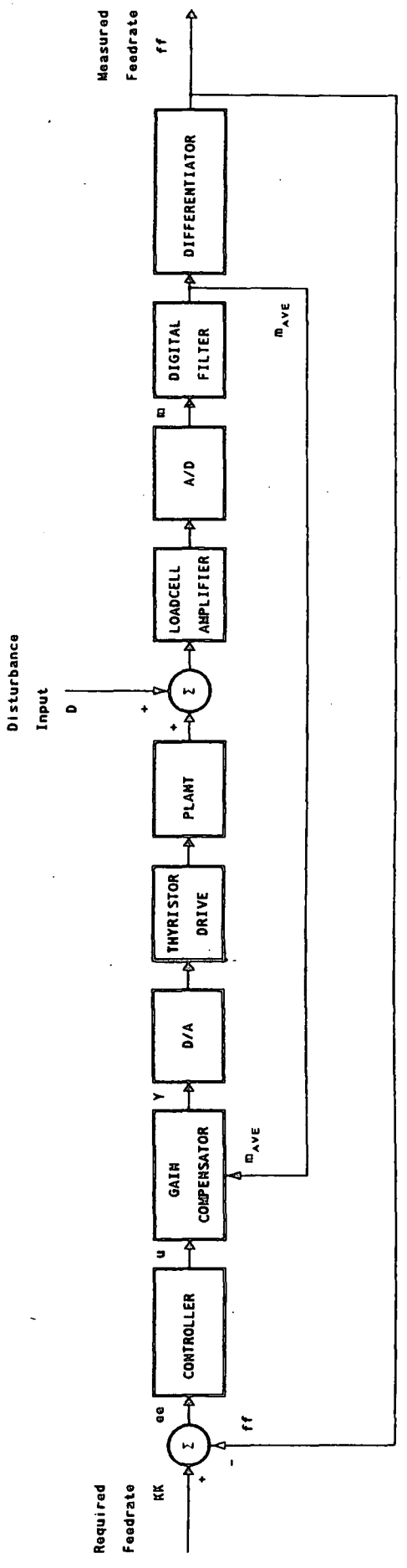

Fig 15. Block diagram of the final configuration.

Chapter four

PLANT IDENTIFICATION AND THE GAIN COMPENSATOR

4.1. INTRODUCTION

This chapter examines the block labelled "plant" in Fig 15 and identifies it as consisting of only an integrator with a non-linear gain term. Once this non-linear gain has been identified an inverse curve is derived and used to modify the plant input. The value of the mass remaining in the hopper is used to select a value on the inverse curve which then modifies the plant input to reduce the value of the overall compensator/plant gain non-linearity.

4.2 PLANT IDENTIFICATION

The complete block diagram of Fig 15 can immediately be reduced, for simplification, to that of Fig 16. Those blocks, for example the "A/D" block, which are simply used to change units or for scaling, can be eliminated.

Because the plant input is a voltage representing the required feedrate of raw material, and output is the weight of the material, the plant must be integral in nature. From observations of the plant in operation so far, it was noted that there is a rapid increase in the feedrate when the whole system reaches a certain mass. This can be clearly seen, for example, in Fig 6 where the plant input is a constant voltage of 205 volts. The slope of a tangent drawn at any instant in time is then the feedrate of the raw material, at that instant. The sudden change in slope indicates that during operation, at a certain mass, it may be considered that there is a rapid

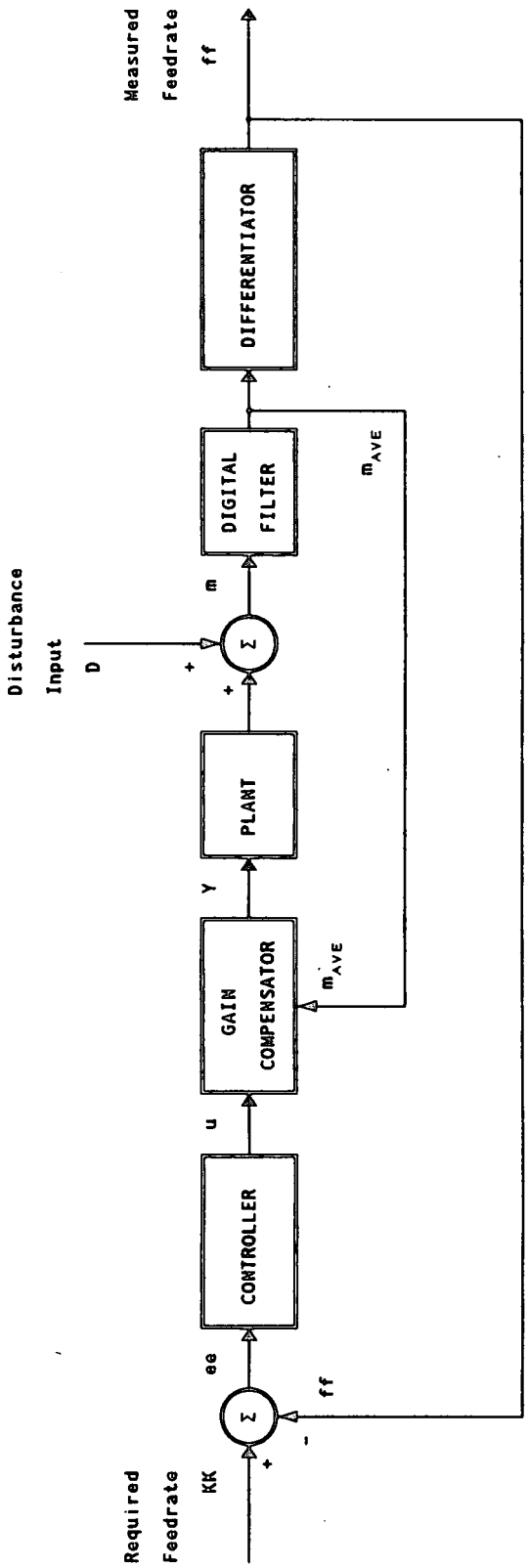

Fig 16. Reduced block diagram.

change in the feedrate and consequently in the plant gain. This is easily understood by considering the damping effect that the raw material has on the vibrating pipe. The assumption is therefore made that the plant consists of an integrator with a gain which is dependent on the mass, and the problem of identification is then one of finding the non-linearity in this gain.

On the basis of the above reasoning the plant is represented, symbolically, by a simple integrator with a non-linear gain as follows :

$$\frac{M(s)}{Y(s)} = \frac{k(m)}{s}$$

with m being the mass of the raw material in the hopper and k(m) the value of the plant gain. The above relation is not entirely mathematically correct. The other symbols are as in the block diagram of Fig 16.

In order to assess the plant gain non-linearity, open loop test runs were carried out. Step changes to the setpoint, during a continuous feed from full to empty were made, and the changing weight of the hopper system recorded. For each setpoint, the feedrate was calculated using the mass fed and time taken and this value used to determine the plant gain. Fig 17 shows these plant gains plotted against the mass (raw material plus hopper mass) at which the gain was calculated.

The curve, as shown in Fig 17, shows the trend in the gain over the complete range of mass values. This curve was obtained by inspection of the gain values and is used to represent the plant gain non-linearity. The outlying low gain points are all the result of very small setpoints. In the mass region below about 15 kg, large setpoints cannot be used because the reduced damping on the feeder pipe would allow very large amplitude vibrations to occur and unstable feeding of the raw material. This

means that the plant gain is not only dependent on the mass remaining in the hopper but that it is also setpoint dependent. The result of the choice of the non-linear gain curve of Fig 17 is that the system will not handle small setpoints very well. The hopper is to feed raw material into a furnace and small feedrates would not be practical.

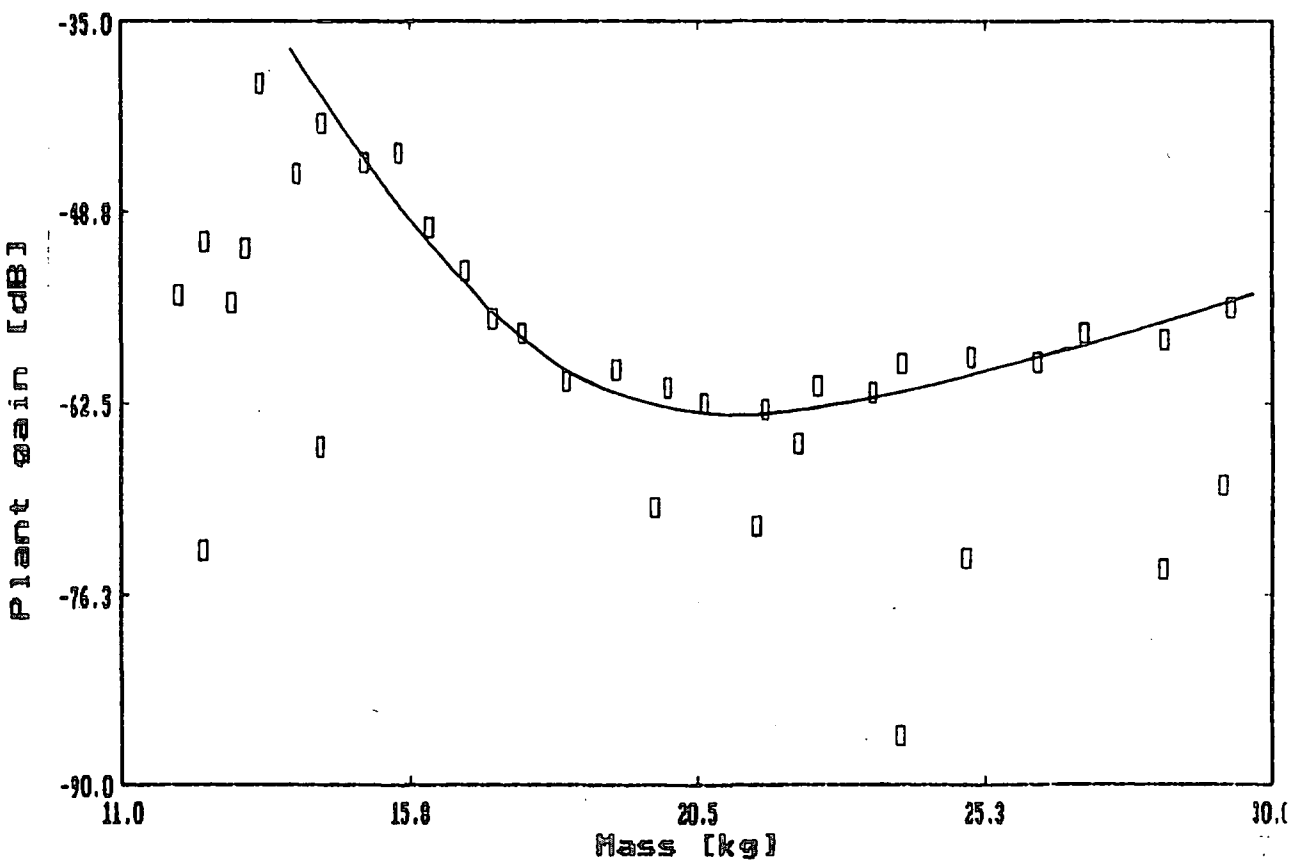

Fig 17. Graph showing the variation in the plant gain against the mass at which the gain was calculated.

4.3 THE GAIN COMPENSATOR

The non-linear gain curve in Fig 17 is simply divided into six straight line segments whose equations are derived. The equations representing the inverse shape were then derived and programmed into a lookup table where the reference is the mass of the raw material. Once again open loop test runs were done to establish the performance of the gain scheduling. Fig 18 shows the response without the gain compensator, for a constant maximum input of 185 volts (see page 11), while Fig 19 shows the response with the gain compensator and the same fixed input.

As can be seen from Fig 19 the non-linearity in terms of the plant gain, shown by sudden changes in slope, although still present, has been substantially reduced when the gain compensator is used.

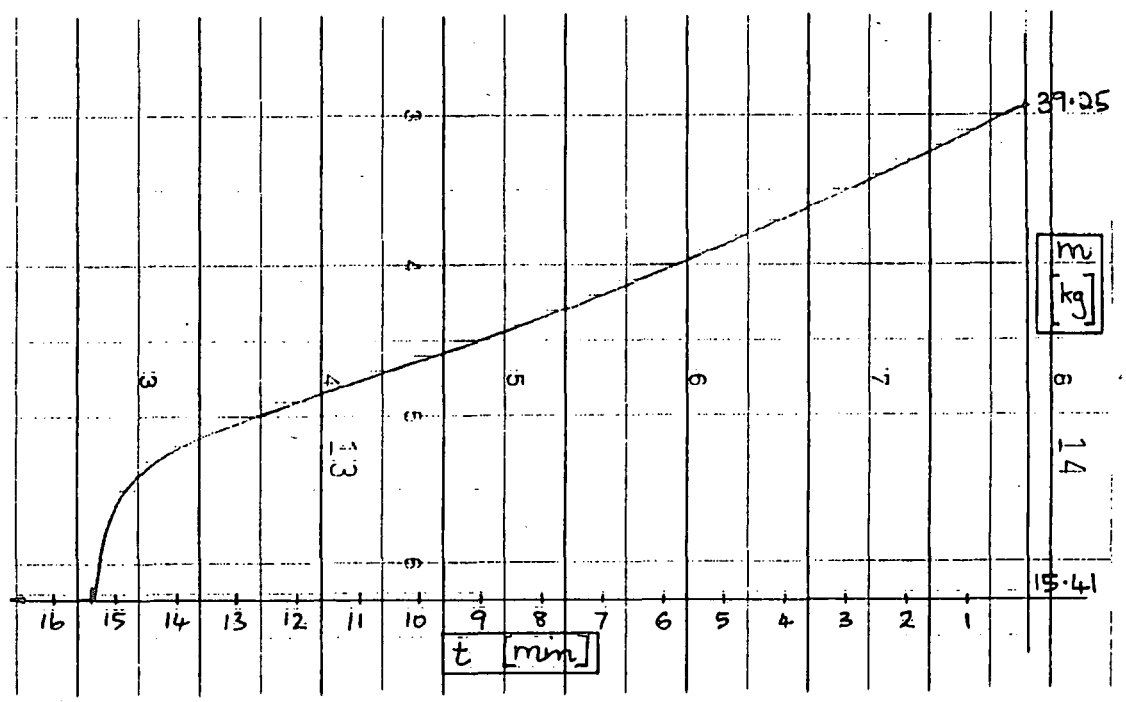

Fig 18. Typical response without gain scheduling.

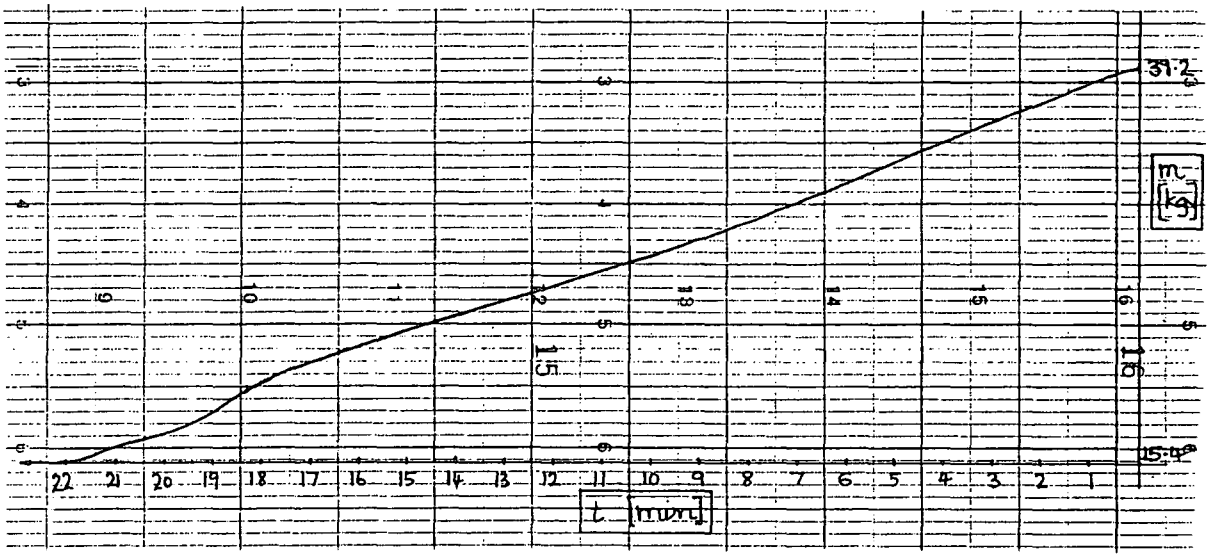

Fig 19. Response with final compensator.

Test runs at lower setpoints showed however that too much compensation was occurring below a mass of 17 kg. This can be clearly seen in the chart shown in Fig 20, for a desired feedrate of 28 kg/hr. Appendix C gives a summary of the responses at other low feedrates. In order to correct for this it was decided to reduce the gain produced by the gain scheduling by an increasing amount, as the setpoint decreases from its maximum value. Two lower values of the setpoint (39 kg/hr and 28 kg/hr) were chosen for the calculation of this additional compensation. The additional compensation would be of the form (Eitelberg 1990):

$$G_{MOD} = G * (a + b*K)$$

where :

	G_{MOD}	= Modified gain
	G	= Normal output gain of the gain compensator
	K	= Setpoint
	a,b	= constant

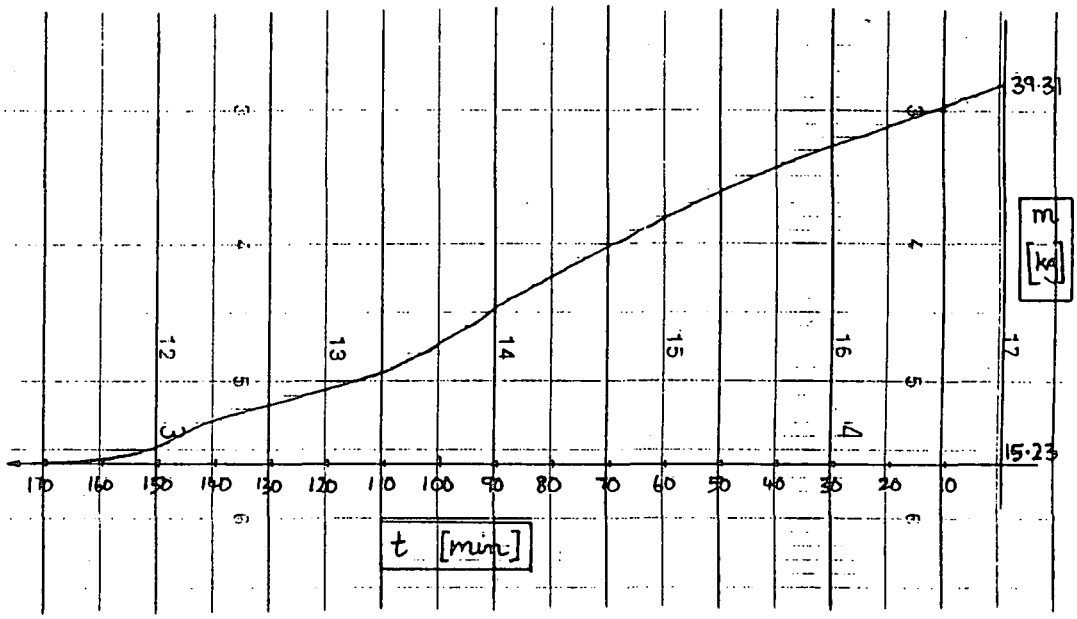

Fig 20. Response with gain scheduling and a feedrate of 28 kg/hr.

Trial and error methods were used to determine the most suitable values of G_{MOD} at the two setpoints. Then a linear least squares approximation method (Underhill 1985) was used to determine the values of a and b, which are as follows :

a = 1.9090909

b = -0.0181818

giving the following :

$$G_{MOD} = G * (1.9090909 - 0.0181818 * K)$$

This equation was then added to the gain compensator in order to provide additional compensation when the raw material remaining in the hopper is less than 17 kg. The amount of this compensation increases as the setpoint decreases away from the maximum value of 50 kg/hr. Once again open loop tests (with setpoints at 50 kg/hr, 45 kg/hr, 39 kg/hr and 35 kg/hr) to measure the performance of the final gain compensator, were done. The results are shown in Appendix C where the maximum and minimum gains over this range of feedrates is 2.69 and 0.238 respectively.

With the gain compensator (that is the original compensator plus the additional

compensation) now considered as a part of the plant and with the assumption that the plant is merely an integrator, its transfer function will be:

$$\frac{M(s)}{U(s)} = \frac{2.69}{s}$$

The value of the gain used in the above equation is taken as the highest measured value because of the fact that the controller is designed for the worst case situation. The design of the controller is done in the next chapter.

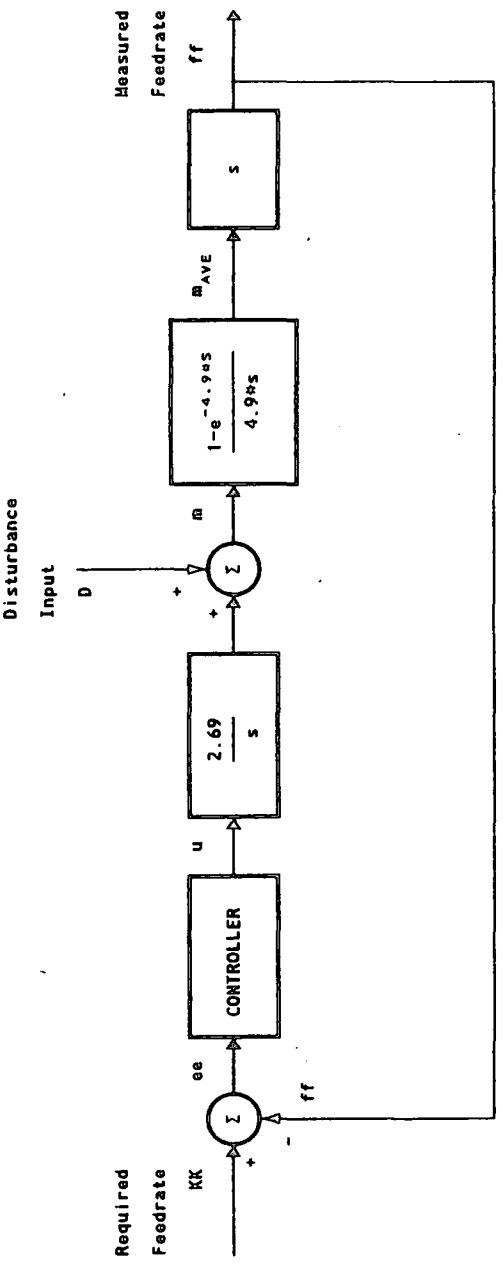

Fig 21. Final block diagram of system.

4.4 CONCLUSIONS

The fact that the plant gain is very non-linear makes acceptable control a very difficult task. It is therefore immediately obvious that a reduction in the plant gain non-linearity will be of great help in the controller design. Gain scheduling has been used to reduce the range of this gain non-linearity, from a value of 51 dB to 21 dB.

The already simplified system block diagram of Fig 16 can now be further simplified to that of Fig 21. The final block to be completed is that of the controller and this forms the basis of the next chapter.

Intentionally blank.

Chapter five

CONTROLLER DESIGN AND TUNING

5.1 INTRODUCTION

The controller is required to ensure good closed loop tracking performance (in order that the output follows the input satisfactorily) while at the same time providing sufficient disturbance rejection (to eliminate the effects of noise). Experience gained on the plant has shown that it is highly susceptible to noise, and as such the disturbance rejection capabilities of the loop are seen to be as important as its tracking ability.

In this work the design of the controller is based on limiting the magnitude of the open loop disturbance transfer function while at the same time ensuring good tracking performance. The inverse Nichols chart (c.f. Horowitz 1963; 1985), or rotated Nichols chart (c.f. D'Azzo and Houpis 1988), are convenient for examining the disturbance rejection capabilities of the system. It allows the open loop transfer function (L) to be plotted, in the normal way, but gives closed loop information about the disturbance transfer function. The design of the controller is done on both the inverse Nichols chart (disturbance rejection) and the Nichols chart (tracking ability). Final tuning is then carried out on the actual plant using test runs over a range of feedrates.

5.2 THE INVERSE NICHOLS CHART

An important advantage in the use of the Nichols chart as a design tool is the fact

that closed loop information is available after having plotted the open loop frequency data. That is, by plotting the open loop transfer function frequency data, $L(j\omega)$, one is able to obtain information about the closed loop response of the system:

$$\frac{L(j\omega)}{1 + L(j\omega)}$$

Referring to the general feedback structure of Fig 22 the disturbance transfer function of the system is:

$$\frac{C(j\omega)}{D(j\omega)} = \frac{1}{1 + L(j\omega)}$$

where $L = GP$ and if the substitution $L = 1/1$ is made then:

$$\frac{C(j\omega)}{D(j\omega)} = \frac{1(j\omega)}{1 + 1(j\omega)}$$

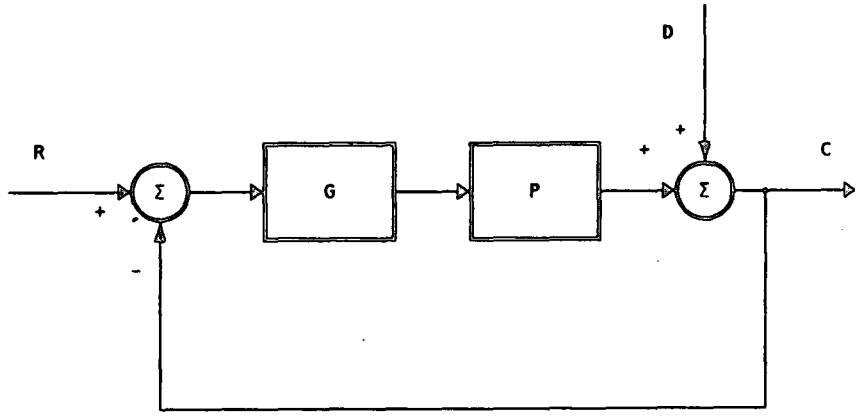

Fig 22. A general feedback structure with a disturbance input.

The conclusion can therefore be made that if the $1(j\omega)$ data is plotted then the closed loop disturbance information will be available. If, instead of the above substitution, the M and N contours of the Nichols chart are inverted, then the closed loop disturbance information will be available after having plotted the $L(j\omega)$ data. This gives rise to the term "inverted Nichols chart" (see Horowitz 1985). The advantage

of using the inverted Nichols chart, is that the plot of the open loop transfer function data does not change. If one is interested in the closed loop disturbance information the inverse Nichols chart is used and if one is interested in the closed loop tracking information then the "normal" Nichols chart is used.

5.3 CONTROLLER DESIGN

Using block diagram manipulation Fig 21 can be redrawn, as shown in Fig 23, where D^* represents a flow rate disturbance.

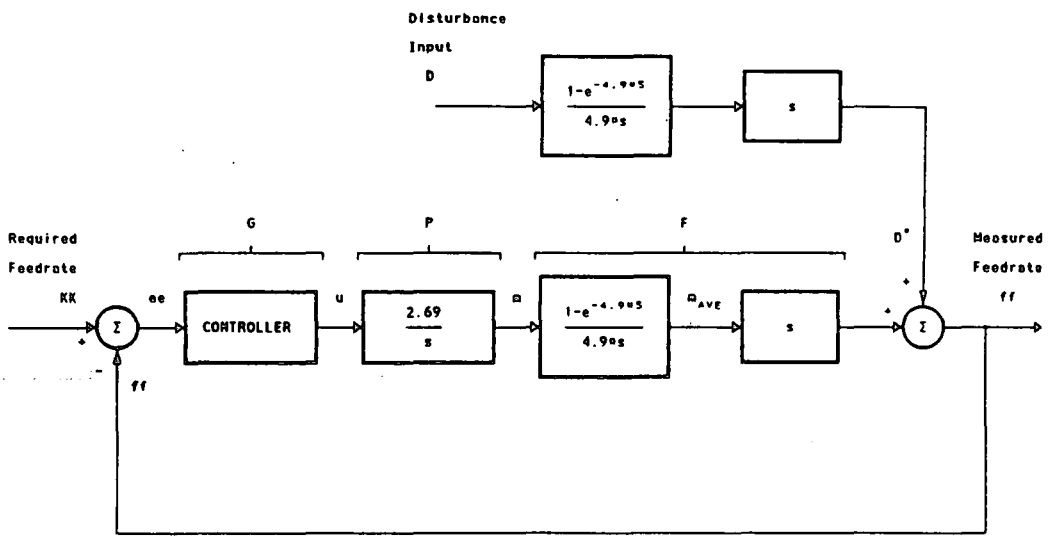

Fig 23. Block diagram of the system.

Now the closed loop disturbance transfer function can be written as:

$$\frac{ff}{D^*} = \frac{1}{1 + L(j\omega)}$$

where:

$$L = G\ P\ F$$

with G being the controller transfer function, P the plant transfer function and F the

filter transfer function (including the differentiator). Now referring to the values shown in Fig 23 the open loop transfer function, without the controller, is given by:

$$L(s) = \frac{0.549*(1 - e^{-4.9*s})}{s}$$

The frequency characteristic $L(j\omega)$, of this transfer function has been plotted on the inverse Nichols chart of Fig 24. Because the chart only covers the range of phase angles from 90° to -270° the response at a frequency of 2 rad/s, and above, is shown at 80° (instead of -280°) and continues through the range of available angles.

The disturbance rejection design objective is to force the magnitude of the disturbance transfer function to be zero or as close as possible to zero. A value of 3 dB, indicated by the 3 dB oval on the inverse Nichols chart, may be considered the maximum acceptable value (Eitelberg 1993). As can be seen from Fig 24 the characteristic's curve actually cuts the 3 dB oval in the 1.1 rad/s frequency region.

From a disturbance rejection point of view the design of the controller must be such as to reduce the open loop gain around the 1.1 rad/s frequency region. One possible way of accomplishing this is by reducing the gain over the complete range of frequencies.

In order to examine what is required of the controller from a tracking point of view, the same open loop frequency response data is plotted on a Nichols chart as shown in Fig 25. It is desirable to have a low frequency closed loop gain of 0 dB. Fig 25 shows that at 0.01 rad/s, 90° of phase lag is required to achieve this.

It is possible to achieve 90° of phase lag with the use of an integrator and the controller gain that results is, in this case, an advantage. The 90° of phase lag that

is added at all frequencies will satisfy the low frequency closed loop tracking gain requirement and by adjusting the gain of the integrator, thereby shifting the response up or down, the +3 dB oval disturbance rejection requirement can also be satisfied.

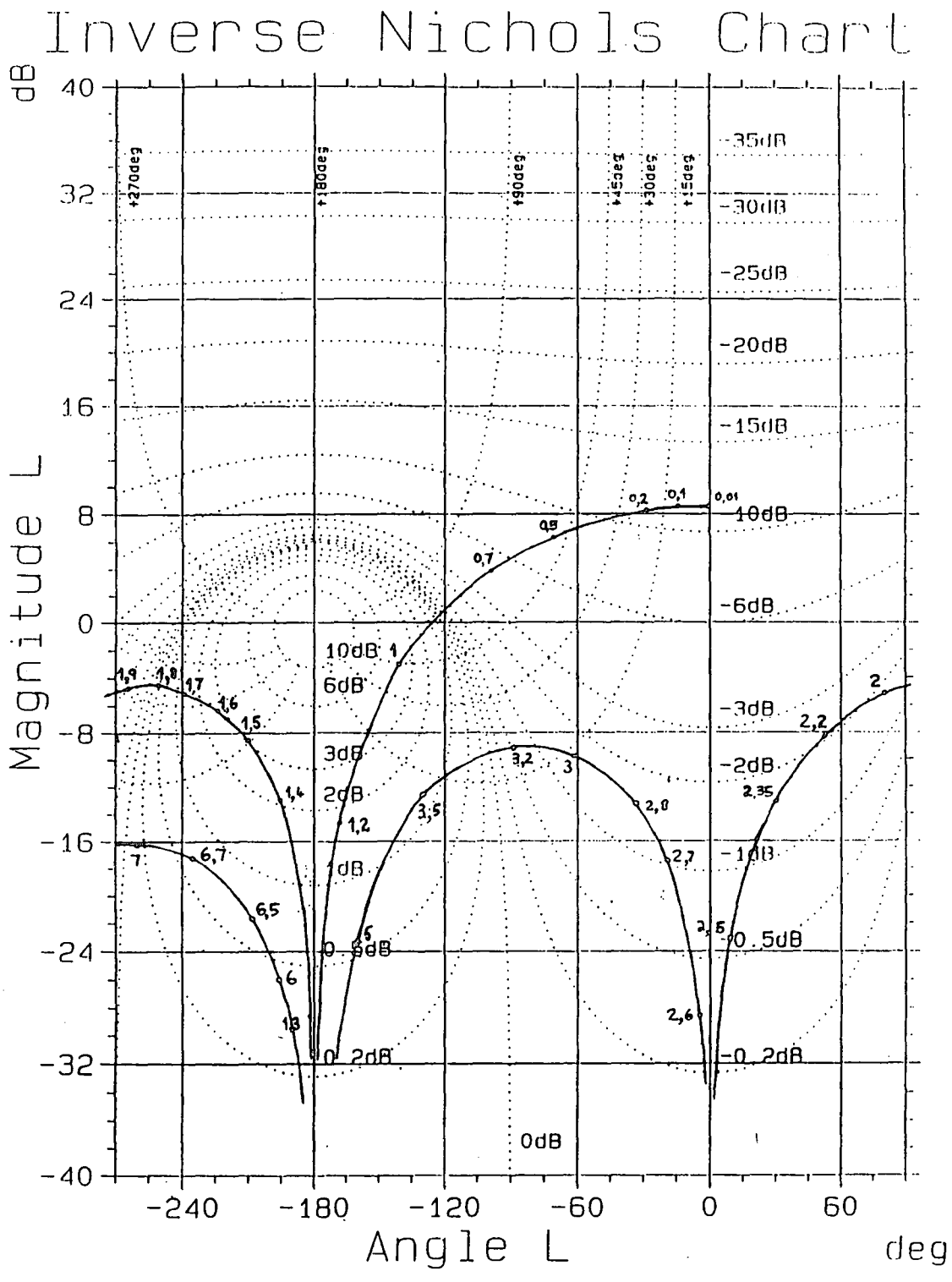

Fig 24. Frequency characteristic without controller, inverse Nichols chart.

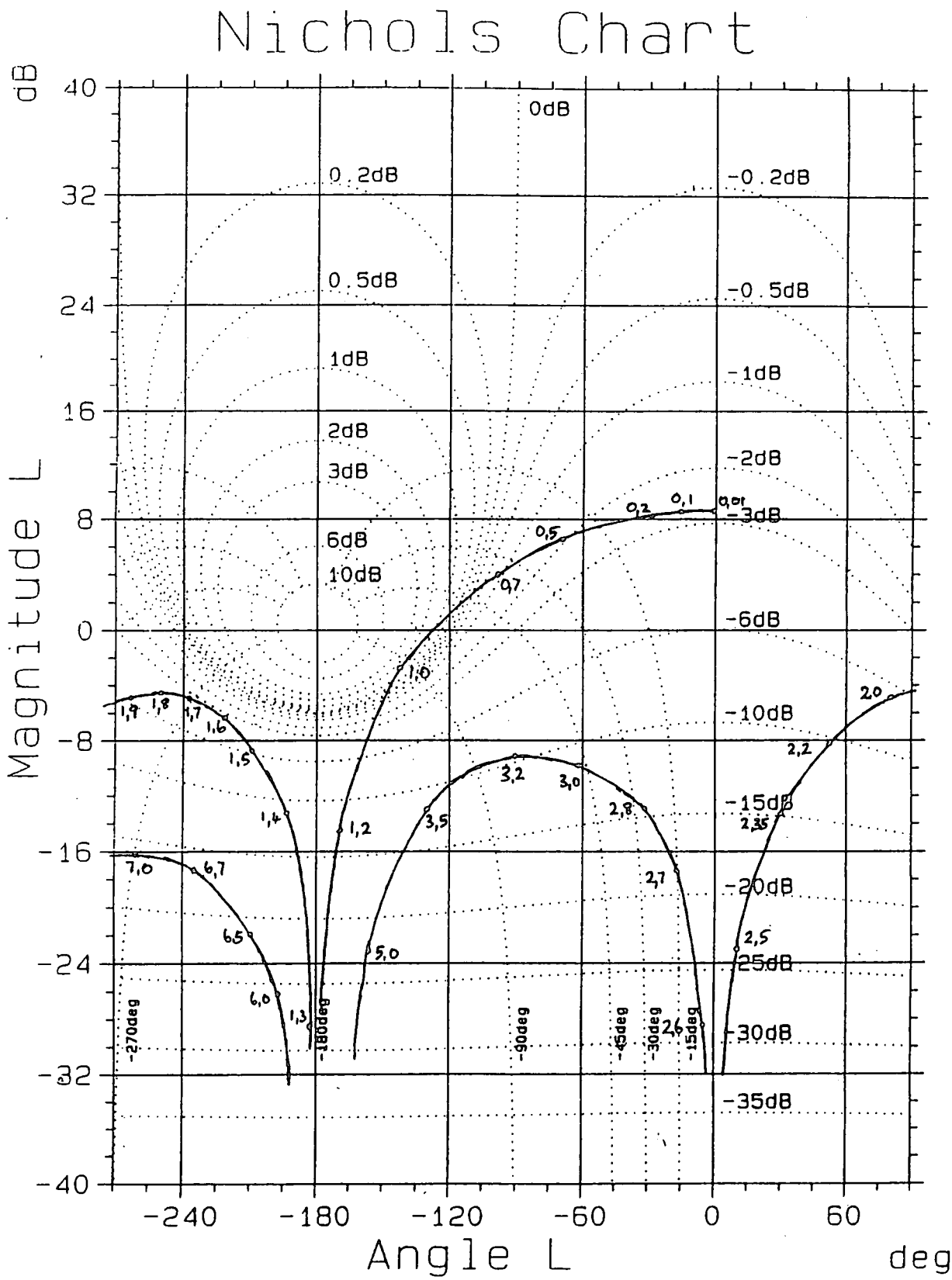

Fig 25. Frequency characteristic without controller, Nichols chart.

When an integral controller is used it is only the gain which is adjustable, so it is convenient to first sketch the open loop transfer function frequency characteristic on the inverse Nichols chart with a 1/s term added, and then to see what amount of gain is required to satisfy the disturbance rejection requirement. Fig 26 shows this response.

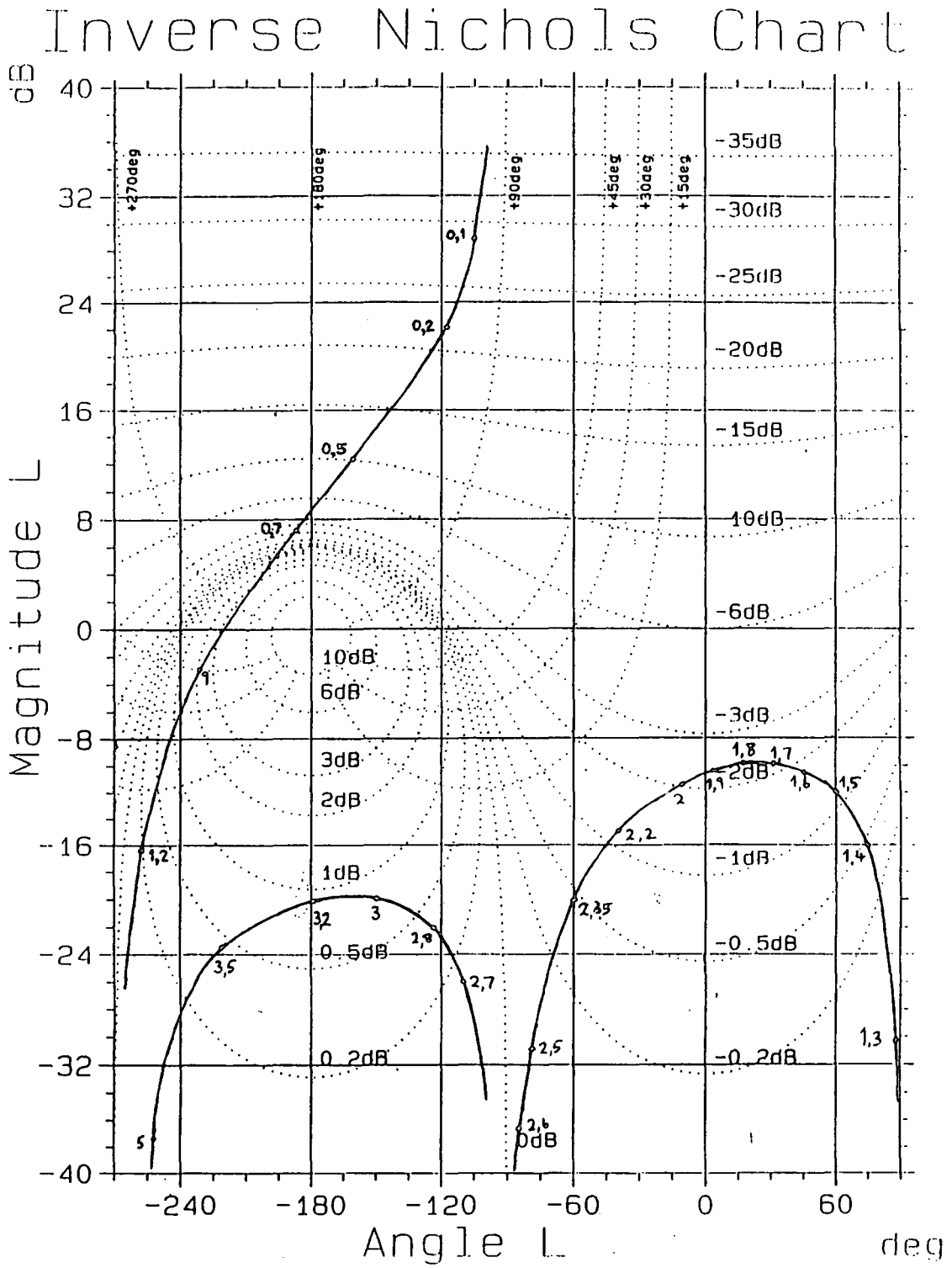

Fig 26. Frequency characteristic with 1/s added, inverse Nichols chart.

As can now be seen, by shifting the response down by 23.5 dB as shown in Fig 27, it will be tangential to the +3 dB oval. Also the characteristic at higher frequencies is forced further downwards and is therefore no longer of any concern as far as disturbance rejection is concerned.

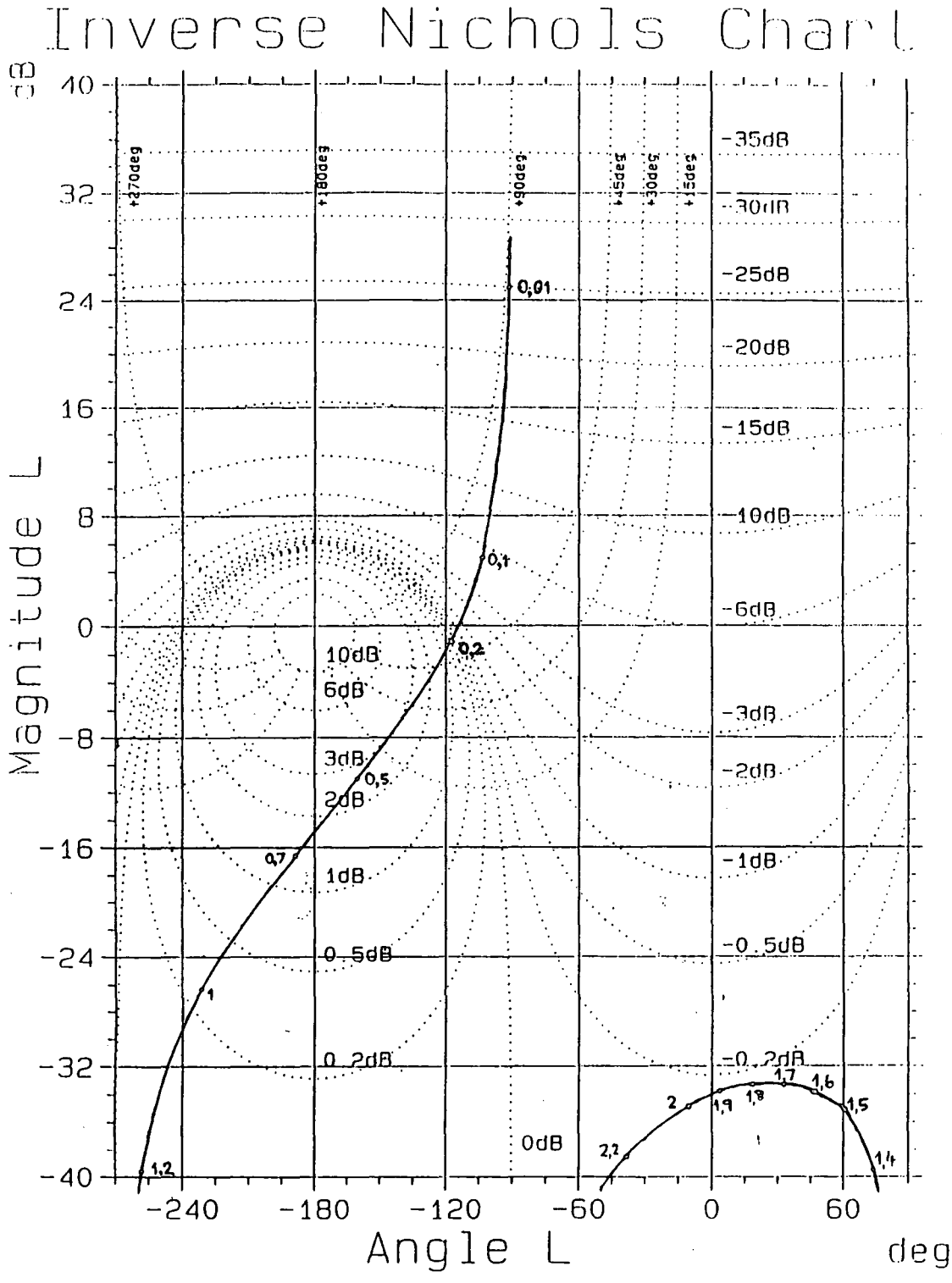

Fig 27. Frequency characteristic with controller, inverse Nichols chart.

This gives the transfer function, $G(s)$, of the controller as:

$$G(s) = \frac{0.0668}{s}$$

and the open loop transfer function now becomes:

$$L(s) = \frac{0.03667*(1-e^{-4.9*s})}{s^2}$$

With the controller designed, essentially on the inverse Nichols chart, the systems tracking ability needs to be verified. The frequency response data of Fig 27 has been transferred to the Nichols chart of Fig 28. The low frequency gain requirement has been satisfied and the gain and phase margins are 15.5 dB and 65° respectively. According to Ogata (1990) these values should be greater than 6 dB and between 30° and 60°, for satisfactory closed loop tracking performance. The values achieved indicate some over correction in terms of the gain. This is due to the oval shape of the closed loop lines. This over correction does allow for an increase in the controller gain of approximately 6 dB and this will allow for the fine tuning of the controller.

5.4 CONTROLLER TUNING

The only adjustment of the controller is in the integrator gain. As explained above the final tuning takes place over a range of 6 dB, that is, increasing the gain from a value of -23.5 dB (or 0.0668 in arithmetic units) to a maximum of -17.7 dB (0.1333). The criterion used for fine tuning, in this work, is the actual performance of the plant and this was done on a trial and error basis while the plant is running. The final value decided upon is for a controller gain of -20 dB (0.1).

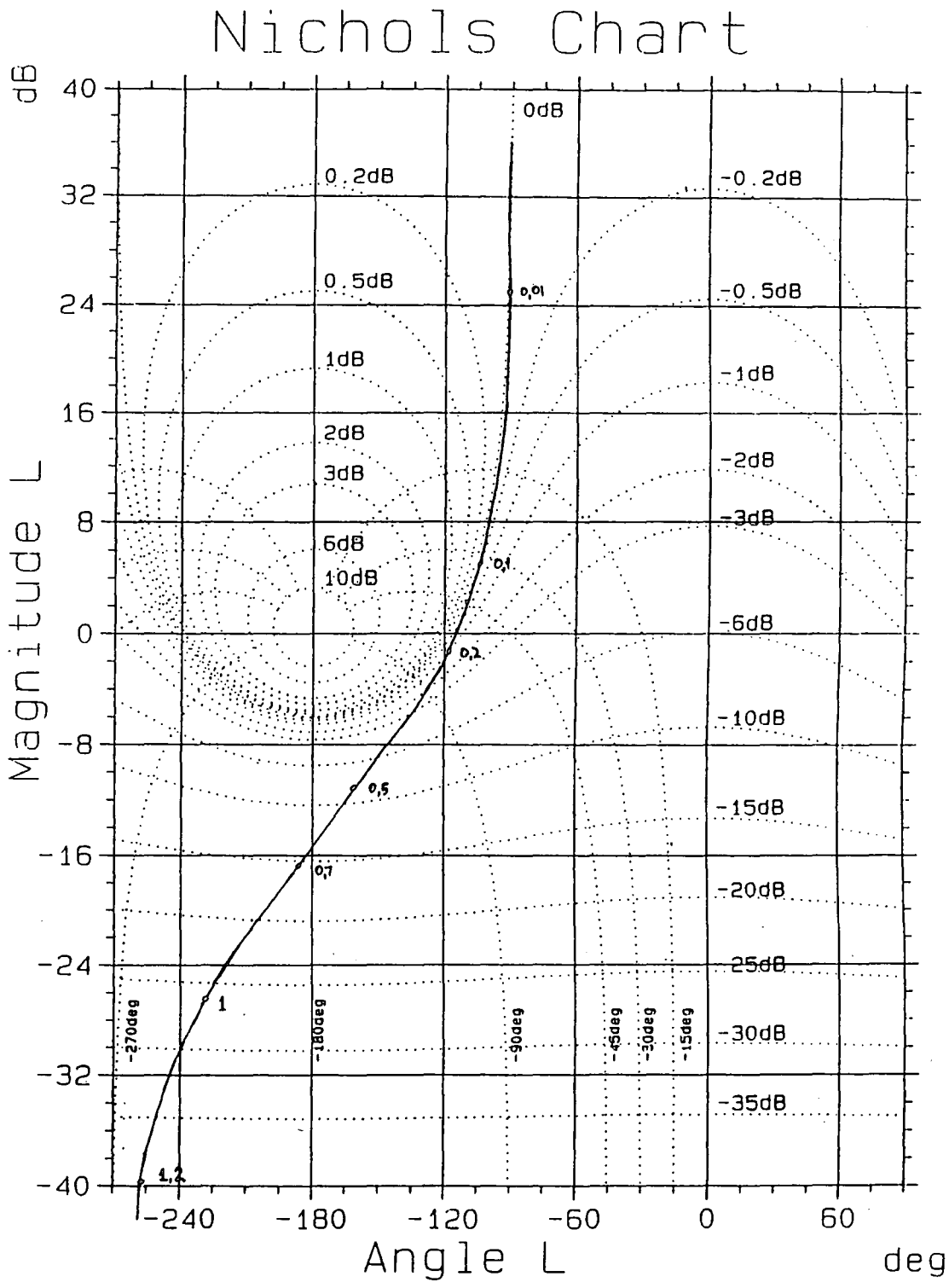

Fig 28. Frequency characteristic with controller, Nichols chart.

5.5 CONCLUSIONS

The final design variable is the gain of the controller and it is because this is set as high as possible that the highest value of plant gain (as mentioned in the previous chapter, page 31) needs to be used. If a value other than the highest value of plant gain were to be used then the possibility would exist of the system being driven unstable when the plant gain went to its maximum value. The design resulted in an arithmetic value for the controller gain in the region 0.0668 to 0.1333 and in the final plant tuning a value of 0.1 was used. This value will result in the magnitude of the closed loop disturbance transfer function to be greater than unity at some frequencies (see Fig 27). This is not considered to be a serious drawback of the resulting controller design because it must be remembered that the controlled variable is the feedrate of the raw material, and large short duration fluctuations in the feedrate can be tolerated.

Chapter six

RESULTS AND CONCLUSIONS

6.1 INTRODUCTION

In the course of this project two separate things were done. In the first place, so called gain scheduling was used in the control of a process made up of a hopper feeding raw material onto a vibrating pipe conveyor. Secondly, quantitative feedback theory, (Horowitz 1963; 1985, D'Azzo and Houpis 1988) was used in the design of the control system for the above type of process.

In this chapter the effect of the filter, with the controller present in the system, is first considered. Then, a comparison of the results obtained with and without the gain scheduling is done to show the improvement in the response achieved when using the gain scheduling.

For illustrative purposes, at the end of the chapter another possible common industrial application of gain scheduling is given.

6.2 RESULTS

With the maximum possible feedrate for a complete batch in the order of 50 kg/hr, three setpoint values, namely, 50 kg/hr, 30 kg/hr and 10 kg/hr were selected to show all the results.

To show the effect of the digital filter the feedrate was recorded at the filter input

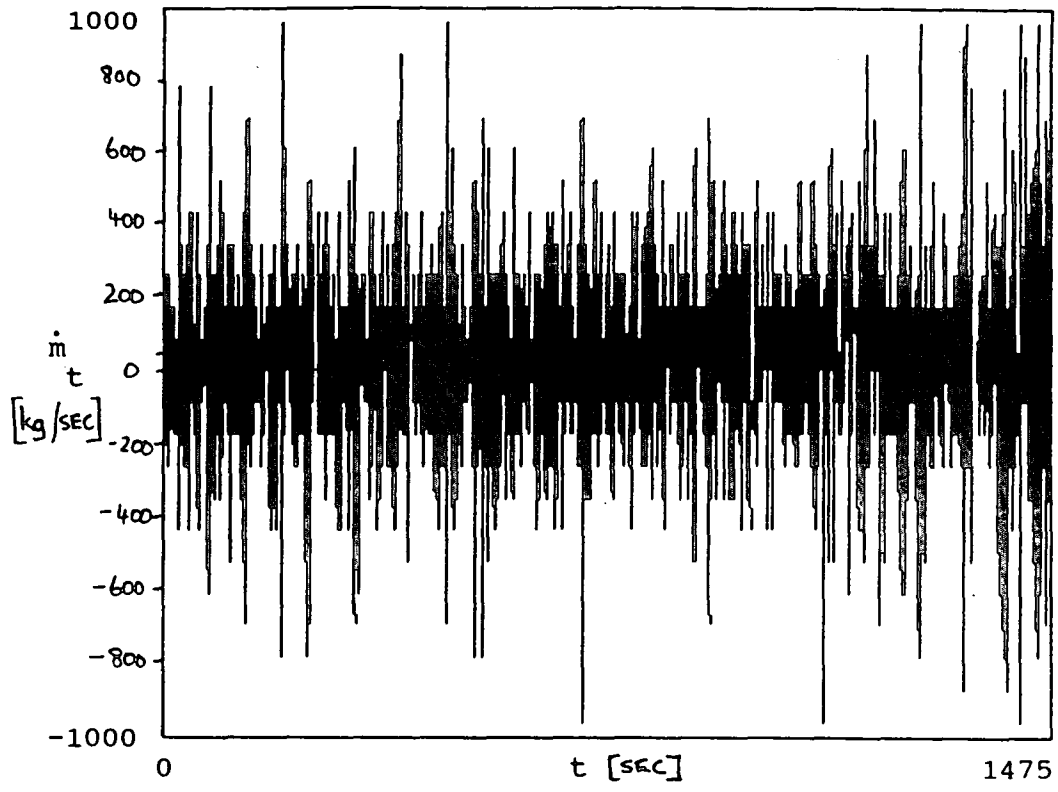

(a)

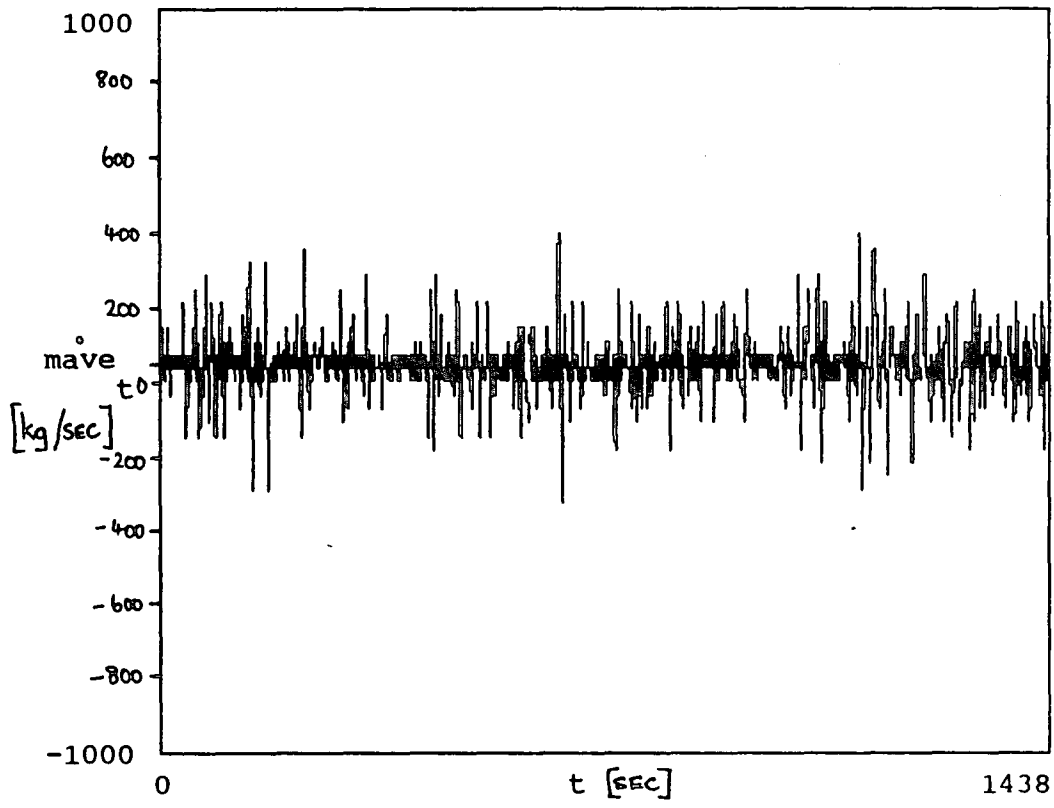

(b)

Fig 29. Feedrate at filter input (a) and output (b), 50 kg/hr.

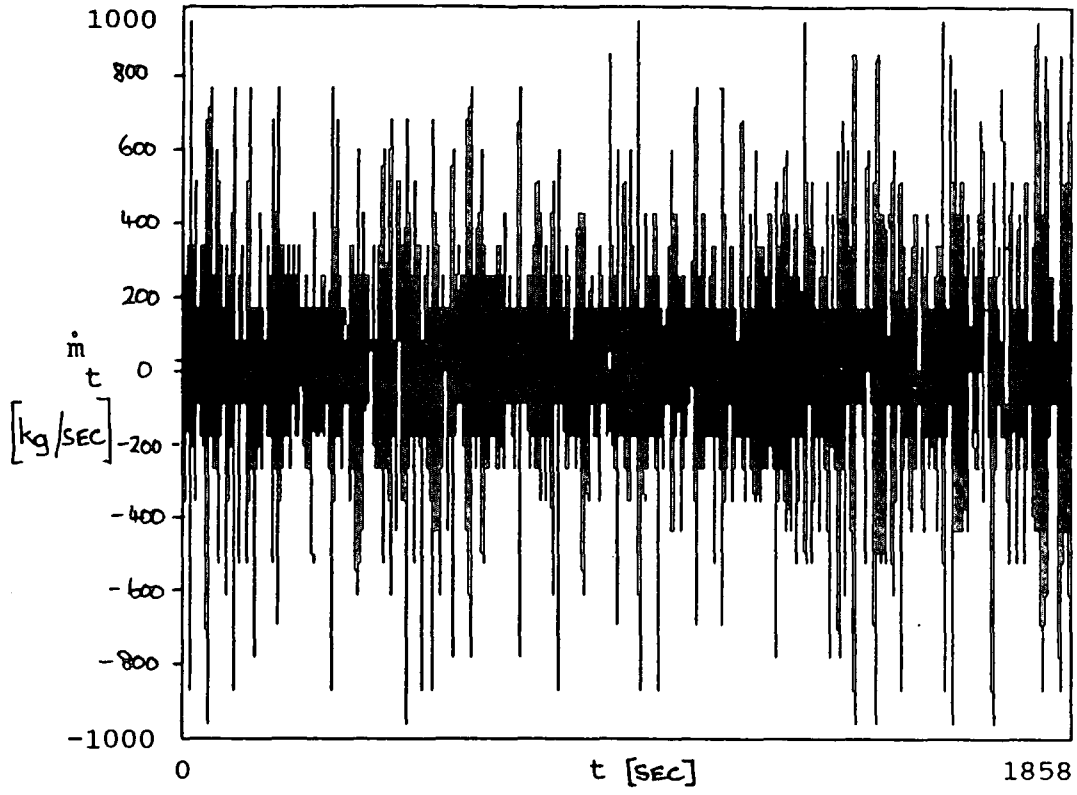

(a)

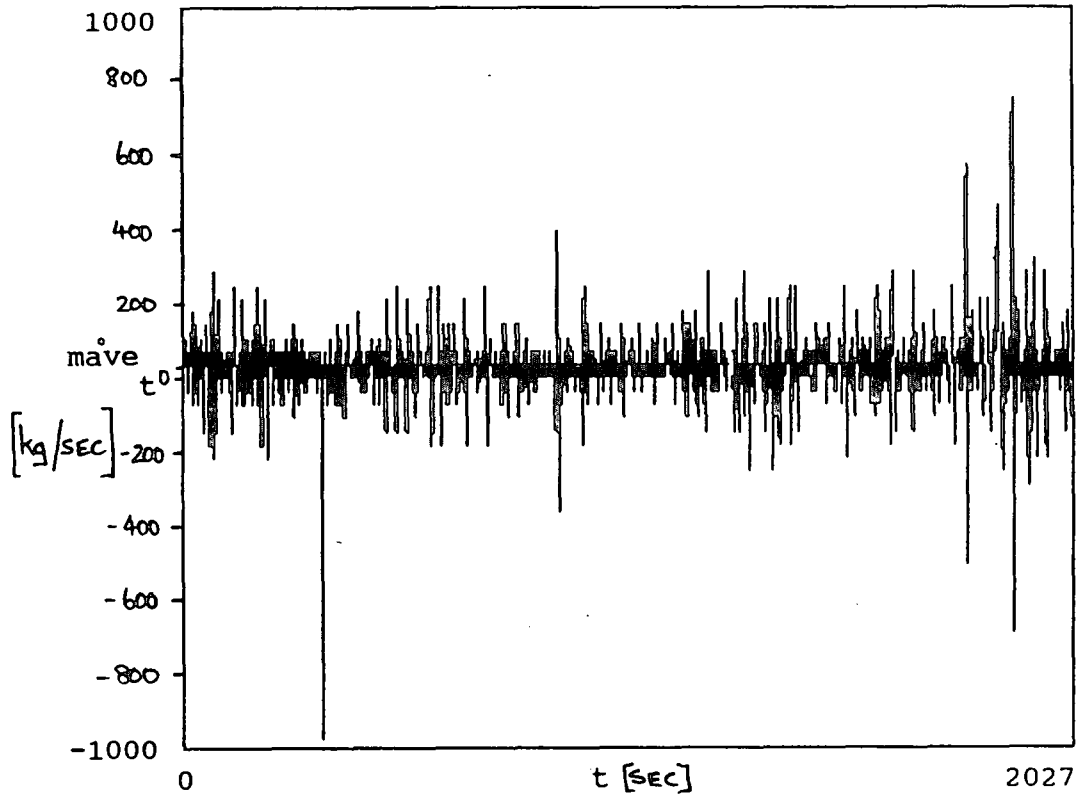

(b)

Fig 30. Feedrate at filter input (a) and output (b), 30 kg/hr.

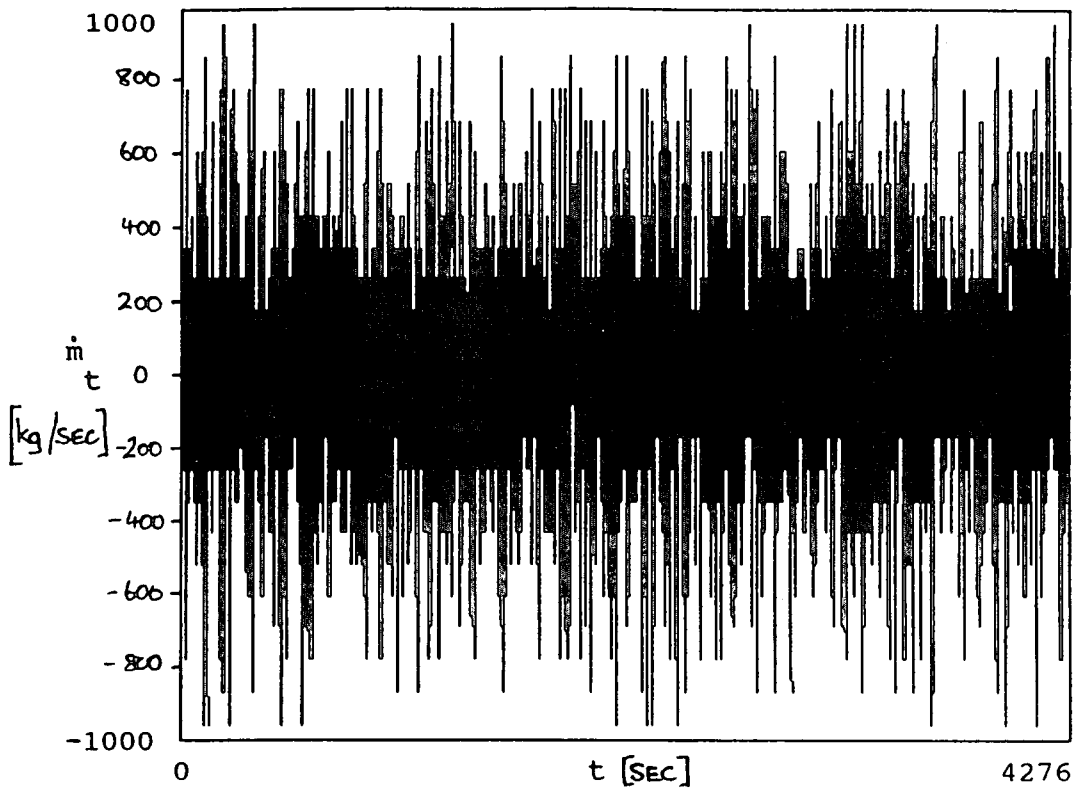

(a)

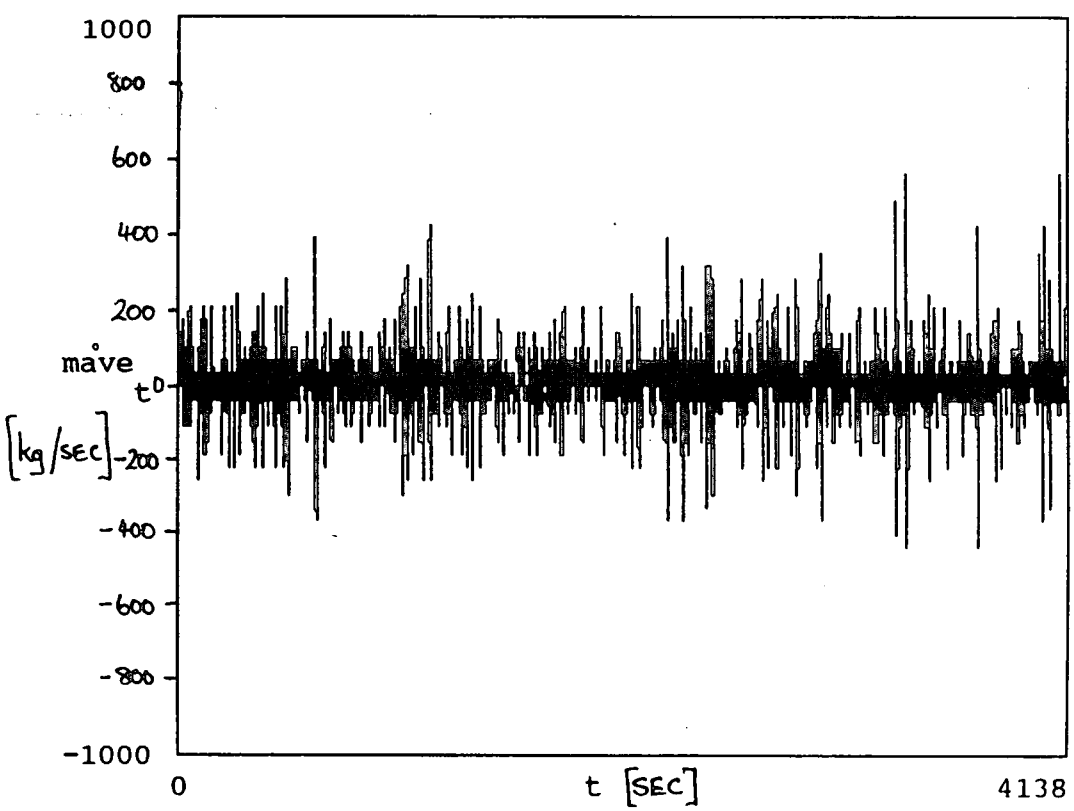

(b)

Fig 31. Feedrate at filter input (a) and output (b), 10 kg/hr.

and output. Fig's 29, 30 and 31 are for the three feedrates where (a) is the feedrate at the filter input and (b) the feedrate at the filter output. In each case the effect of the filter is obvious. The vertical axes represent the feedrate and their scales have deliberately been kept the same; time, in seconds, is plotted on the horizontal axis. This does however make it difficult to distinguish either the zero line or the feedrate setpoint line. One further important point is evident from these diagrams. At low feedrates, illustrated here at 10 kg/hr, the plant gain increases significantly. This increased gain amplifies the noise as can be seen in both diagrams of Fig 31. This fact is important in the discussion later in this chapter.

Because of the resolution problems of the above diagrams and the difficulty of extracting useful information about filter performance, the filtered mass data are displayed against time. This is shown, for the three feedrates, in Fig's 32, 33 and 34 respectively, where part (a) is with the gain scheduling in place and part (b) is without the gain scheduling. It must however be remembered that it is the feedrate that is the control variable and not the mass. This means that it is the slope of the response (which is the feedrate) that is of importance.

In order to assess the advantage gained by the use of the gain scheduling it is replaced with a fixed gain equal to the minimum that would be set by the gain scheduling for that particular feedrate. This is done by setting the value of G, in the procedure "SETGAIN" in the software, to its lowest possible value for each particular feedrate (see the program listing on page 67). This is considered fair for comparison purposes because it removes any advantage that would be gained by using the gain scheduling. The controller is left unaltered.

Fig 32(a) shows that with about 12 kg remaining in the hopper saturation of the

controller output occurs. One of the variables monitored during operation was the controller output and this confirmed the saturation. This is seen by the decreasing of the slope and therefore the feedrate. The controller does however recover and once again achieve the required feedrate. This is shown by the two parallel dotted lines. The feedrate calculated from these lines is 50.27 kg/hr. Because of this saturation 50 kg/hr is considered to be the maximum continuous (over a complete batch) feedrate that can be achieved. It must however be remembered that much higher feedrates are possible, when the hopper has only a small amount of raw material in it.

Fig 32(b) shows the effect of both saturation of the controller output and a reduction of the loop gain with the gain scheduling removed. Once again the dotted line shows the feedrate setpoint which is achieved towards the end of the batch.

Fig 33 shows the results at a feedrate of 30 kg/hr, where (a) shows that the controller is able to quickly restore the feedrate to its setpoint value. There was a large disturbance near the end of the test run after which the control system easily maintained the feedrate. The calculated feedrate is 29.115 kg/hr. Fig 33(b) shows a similar effect to that of Fig 32(b) where the calculated feedrate is 28.52 kg/hr.

Fig 34 is for a feedrate of 10 kg/hr where the increased noise levels (see Fig 31 and the related discussion on page 49) are obvious. No positive conclusions can be drawn for this feedrate. The control system design was done for higher feedrates (mainly 30 kg/hr and greater) for several reasons. Firstly, the change in mass of the system at low feedrates is very slow, and therefore difficult to measure. Secondly, the time taken for a complete batch was too long and impractical. Thirdly, the mechanical design is not suited to measuring small masses (a 50 kg loadcell is used).

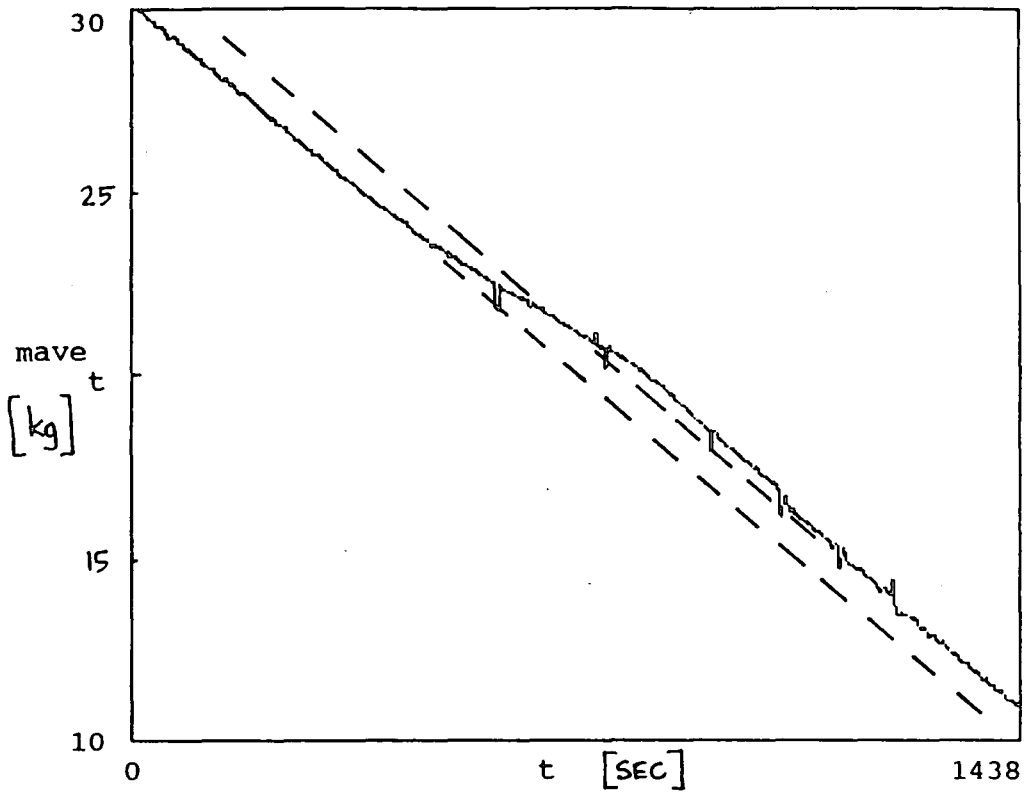

(a)

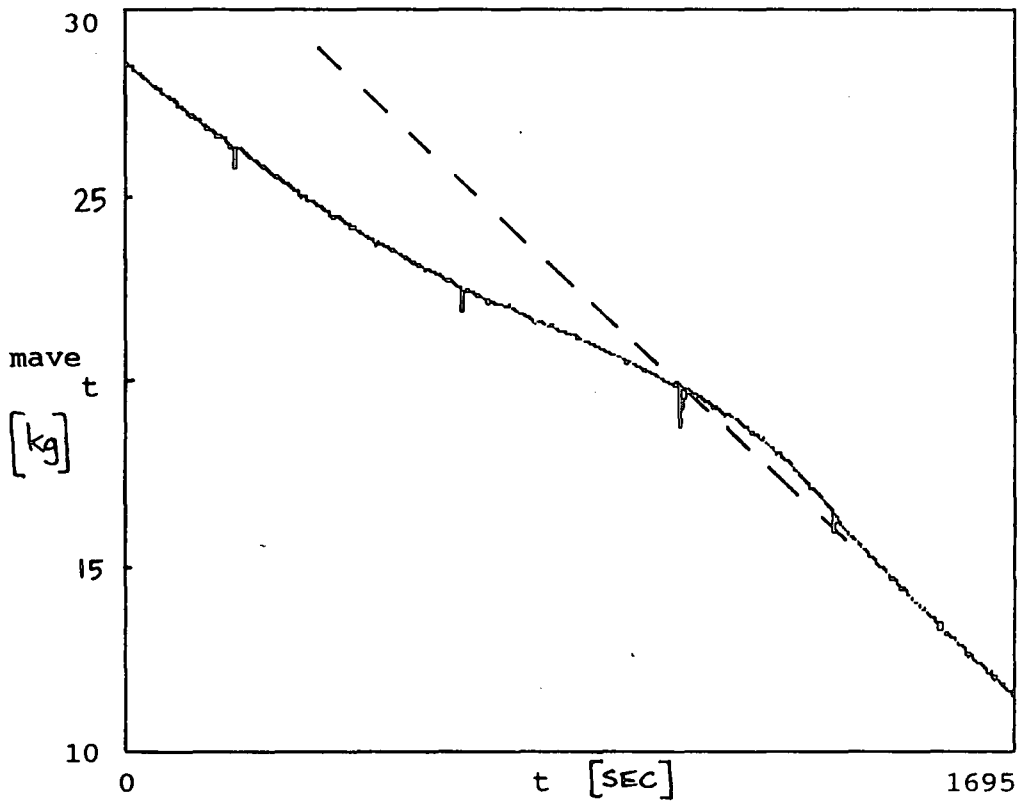

(b)

Fig 32. Mass change with (a) and without (b) gain scheduling, 50 kg/hr.

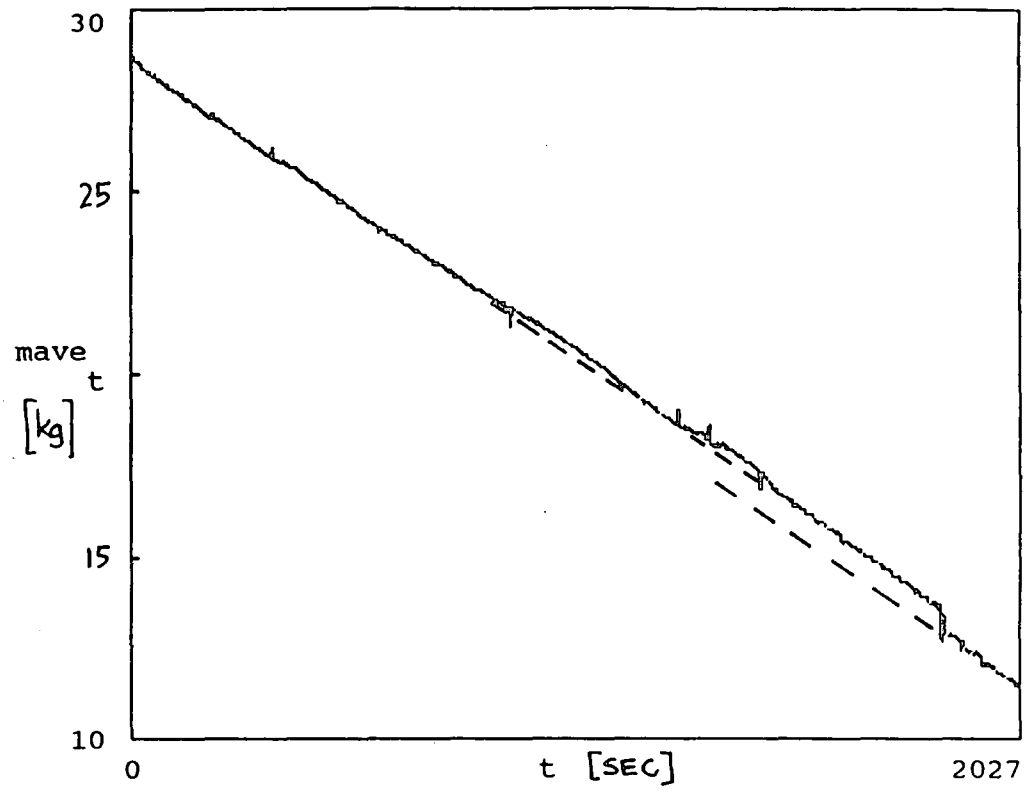

(a)

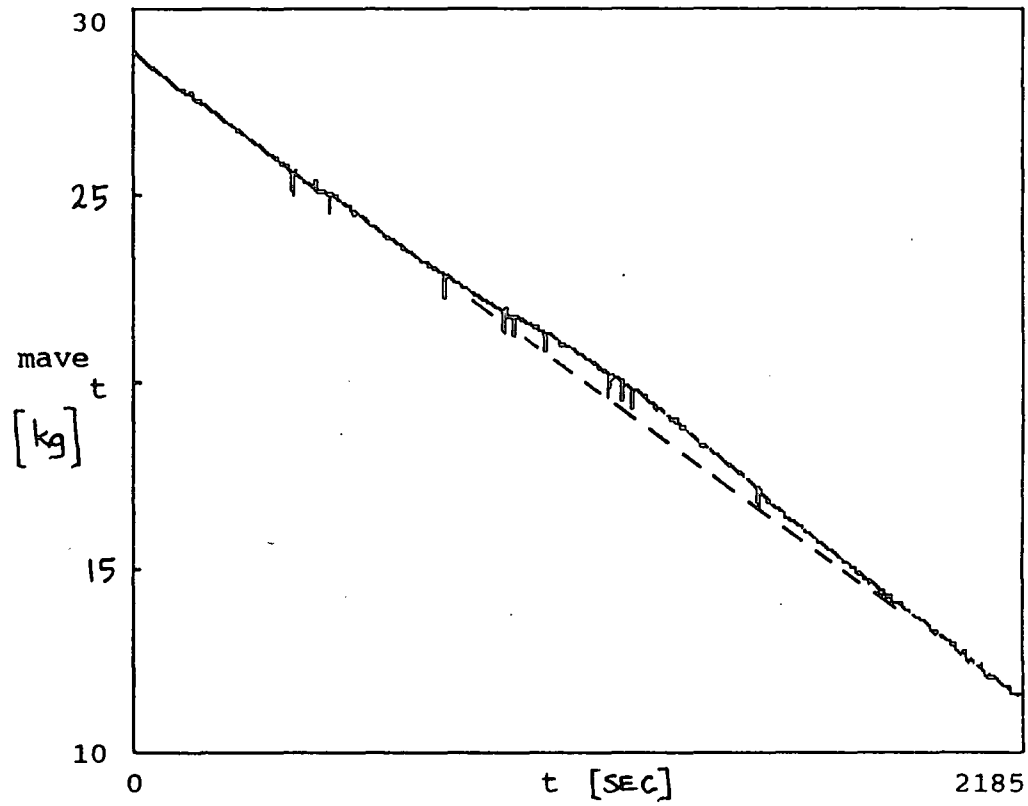

(b)

Fig 33. Mass change with (a) and without (b) gain scheduling, 30 kg/hr.

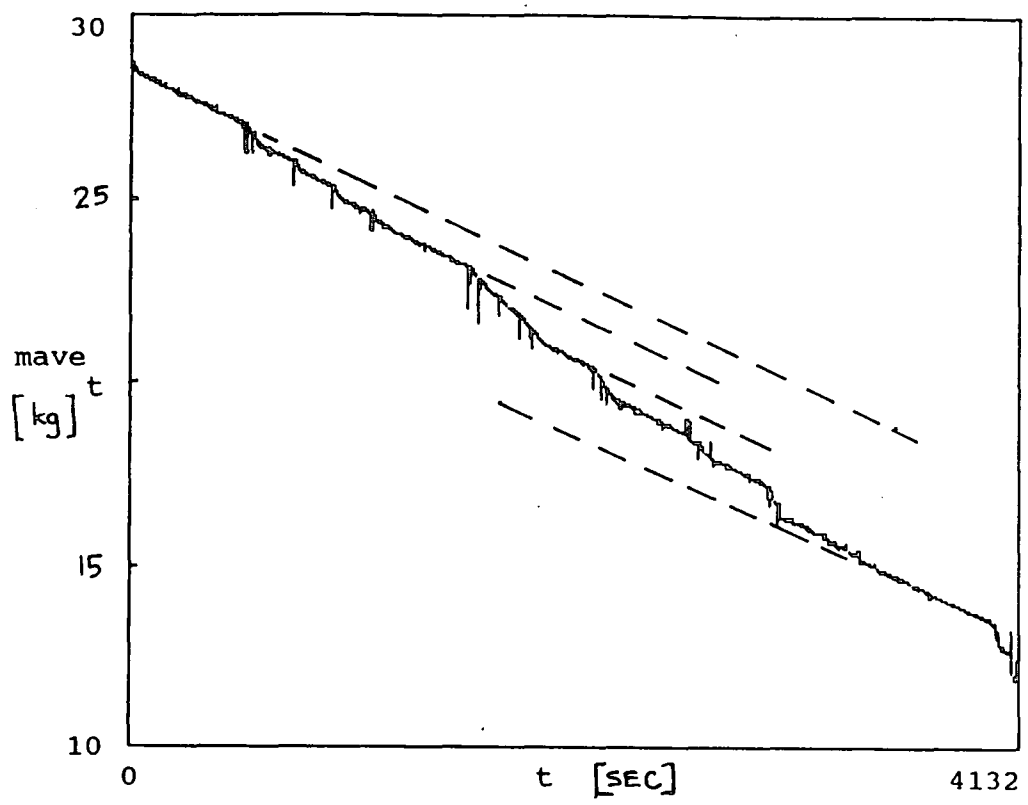

(a)

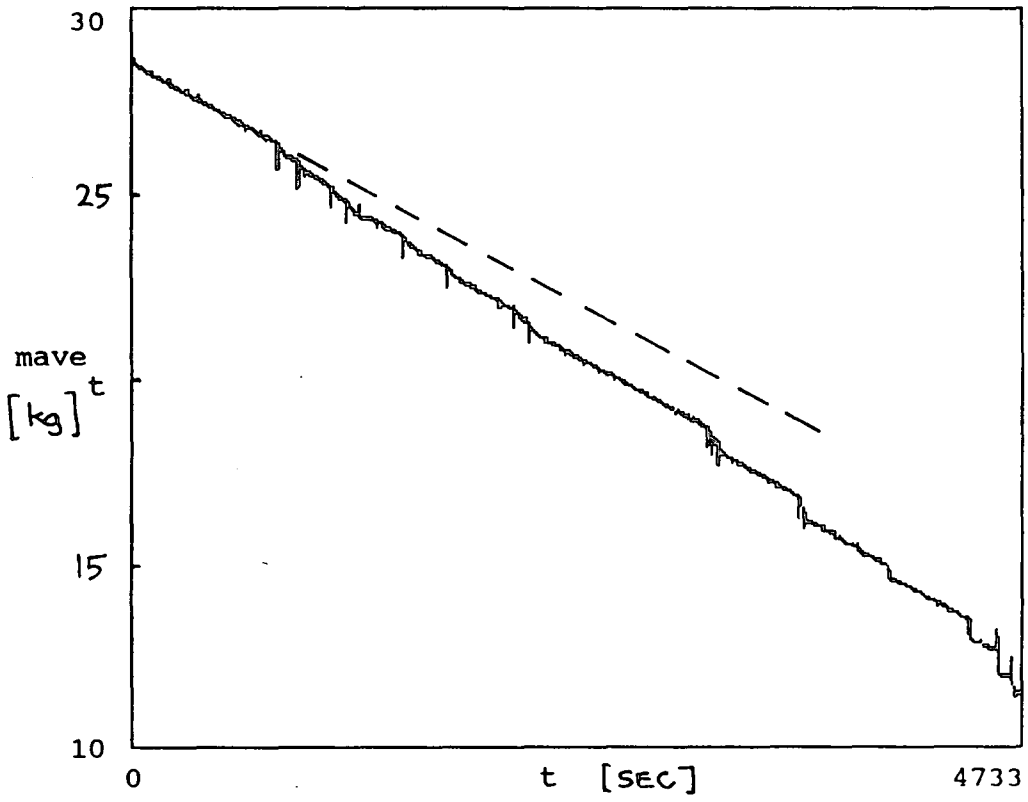

(b)

Fig 34. Mass change with (a) and without (b) gain scheduling, 10 kg/hr.

6.3 CONCLUSIONS

Finally, it is again emphasised that the design here is to control the feedrate of raw material and not the amount of material fed. This makes the recovering of the slope of the line in Fig's 32, 33 and 34 of importance. If it was desired to control the amount of material fed then a recovery to the initial dotted line in each case would be important. From the point of view of the control system, the only change that would need to be made would be to compare the masses rather than the feedrates. This is quite easily achieved, through block diagram manipulation (and referring to Fig 21), by moving the differentiator to the required feedrate input side of the first summing junction. There it will become an integrator and a comparison of the masses can be done. Fig 35 shows these changes. There will be no need for further design work. The controller now becomes a proportional one with a gain of 0.1. This is the way in which control is achieved in the controller designed by Mintek (Nicol *et al.* 1986). Here the mass signal is forced to follow a linear ramp signal in time.

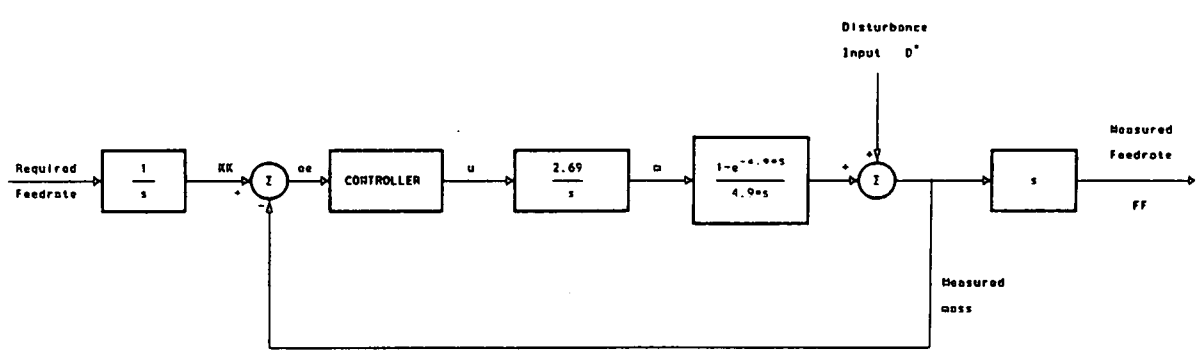

Fig 35. Block diagram showing the comparison of masses rather than feedrates.

The use of gain scheduling is perhaps not a new idea but its application to this type of plant shows obvious advantages. There are many other industrial plant applications in which the dynamics can be ascribed, mainly, to a non-linearity of the gain. One such situation is the control of liquid level in a tank. If the control is done using a valve in the outflow pipe, then as the setpoint is changed so that the head pressure across the valve changes and consequently the actual flow through the valve changes. Gain scheduling could quite successfully be applied here, where the value of the gain would be dependent on the level in the tank.

References

BARCZA, N. and STEWART, A.B. The potential of Plasma-arc technology for the production of ferro-alloys. Paper presented at the 3th International Ferro-alloys Congress (INFACON 83), Tokyo. 1983, pp. 82-90.

D'AZZO, J.J. and HOUPIS, C.H. Linear Control System Analysis and Design, Conventional and Modern, 3rd ed. New York: Mc Graw-Hill. 1988.

EITELBERG, E.E. Numerous personal discussions and explanations. 1988-1993.

Encyclopeadia of Chemical Technology, 3rd ed, v.11. New York : John Wiley and Sons Incorporated. 1980.

HOROWITZ, I. Synthesis of Feedback Systems. New York: Academic Press. 1963.

HOROWITZ, I. Robust Control. Unpublished lecture notes. University of Natal, Durban, Department of Electrical Engineering. 1985.

JAY, H. Filters. Unpublished lecture notes. Technikon Natal, Durban, Department of Electronic Engineering. 1986.

Materials and Technology/ edited by T.J.W. van Thoor, v.3. London : Longman Group Limited. 1970.

NICOL, K., RENNIE, M., and STEWART, A.B. The control and operation of a pilot-plant d.c. plasma furnace. Paper presented at the 4th International Ferro-alloys Congress (INFACON 86), Rio de Janeiro. 1986, pp. 179-188.

OGATA, K. Modern Control Engineering, 2nd ed. Englewood Cliffs: Prentice-Hall. 1990.

Process instruments and controls handbook/ edited by D.M. Considine, 2nd ed. New York: McGraw Hill Book Company. 1974.

RODD, M.G. and RABEY, C.C. A computer based system for the evaluation of electric fields in a model submerged arc furnace. Automation in Mining, Mineral and Metal Processing/ edited by F.H. Lancaster. Pretoria: South African Council for Automation and Computation. 1977.

SHINSKEY, F.G. Shinskey on control. SA Measurement and Control, June, 1984, pp.26.

SOUTH AFRICAN IRON AND STEEL CORPORATION. Steel in South Africa. Published on the occasion of the silver jubilee of the South African Iron and Steel Corporation Limited. 1953.

STEWART, A.B. Mintek internal memorandum, untitled. 1986a.

STEWART, A.B. Numerous telephonic discussions. 1986b.

UNDERHILL, L.G. Introstat, 4th ed. Cape Town: Juta and Company Limited. 1985.

Appendix A

This appendix is a summary of the results of the test runs done to determine the best positions of the two mechanical variables. Because of the fact that the feedrate changes rapidly, at a certain mass, as the hopper is emptied, the feedrate and deviations from this feedrate are done from full to approximately 23 kg in each case. The charts appear backwards but this is merely due to the fact that they were done using a continuous paper chart recorder. Table 1 on page 14 gives a summary of the test runs and the deviations.

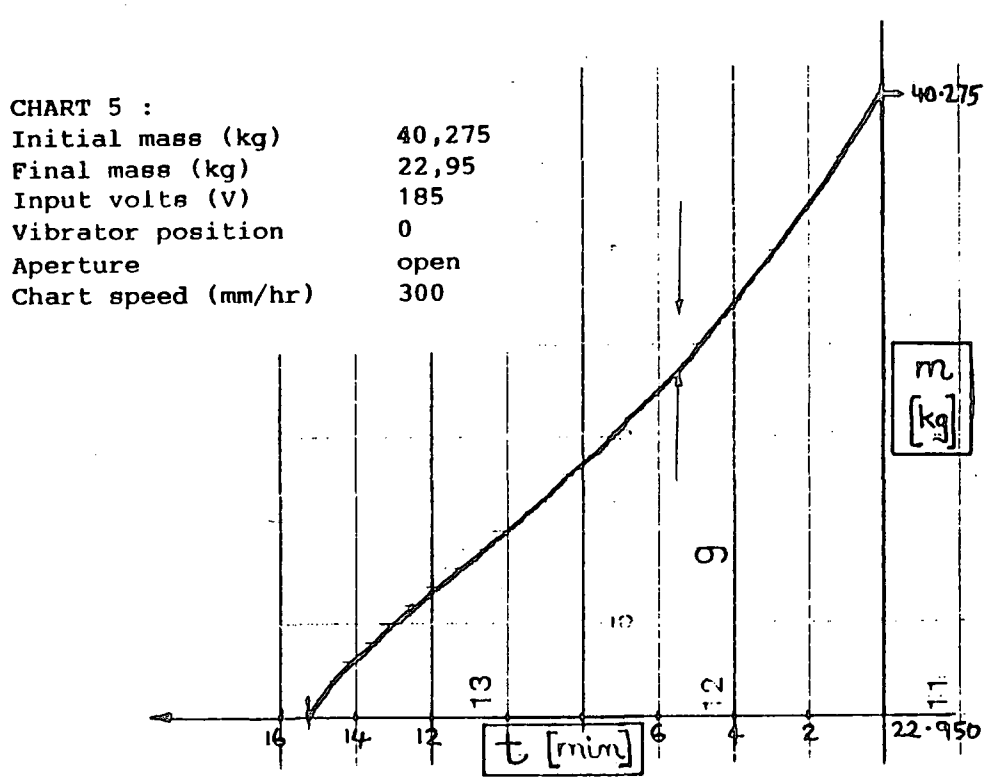

Chart 5. Vibrator position - 0, aperture - open.

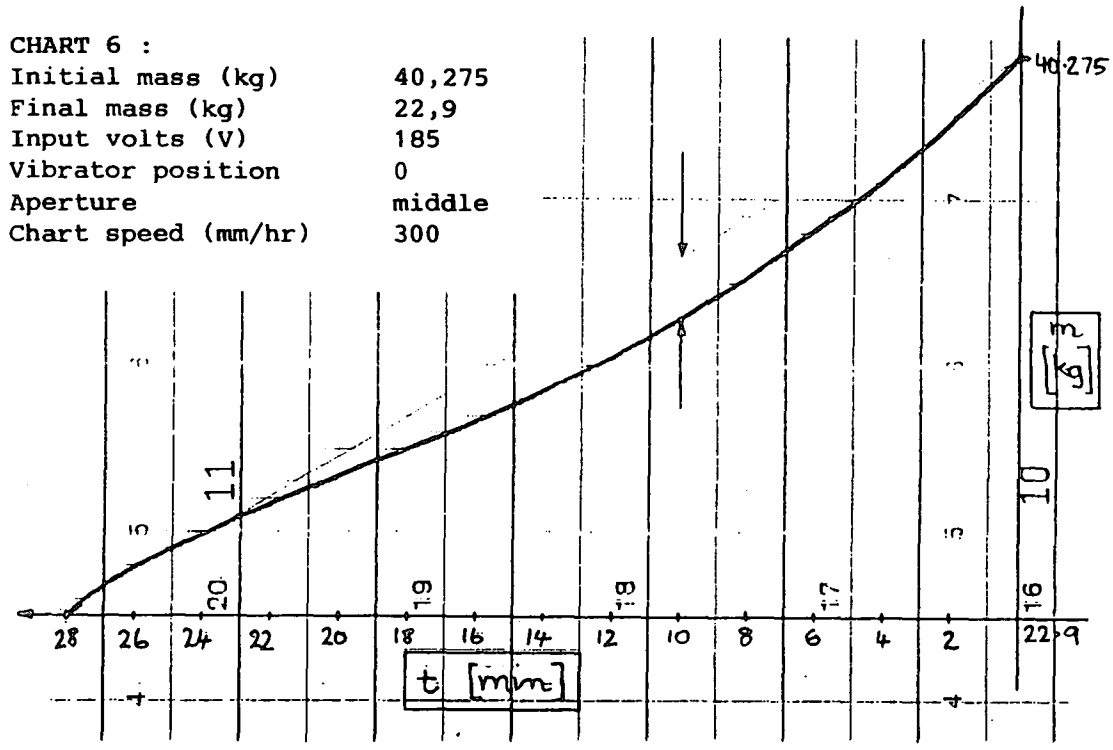

Chart 6. Vibrator position - 0, aperture - middle.

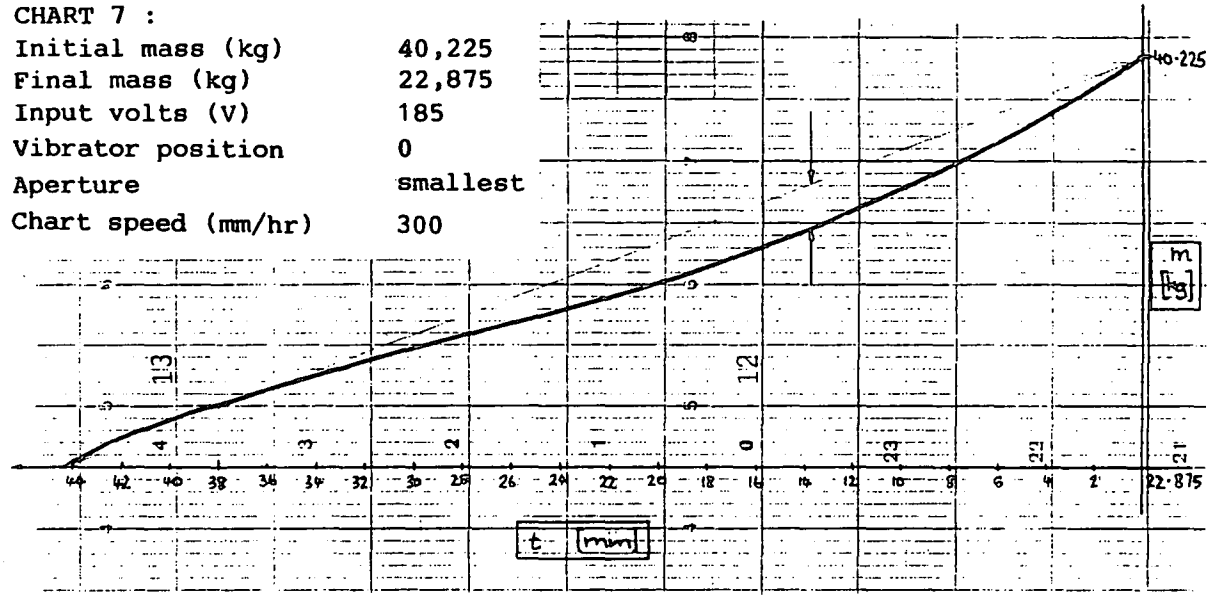

Chart 7. Vibrator position - 0, aperture - smallest.

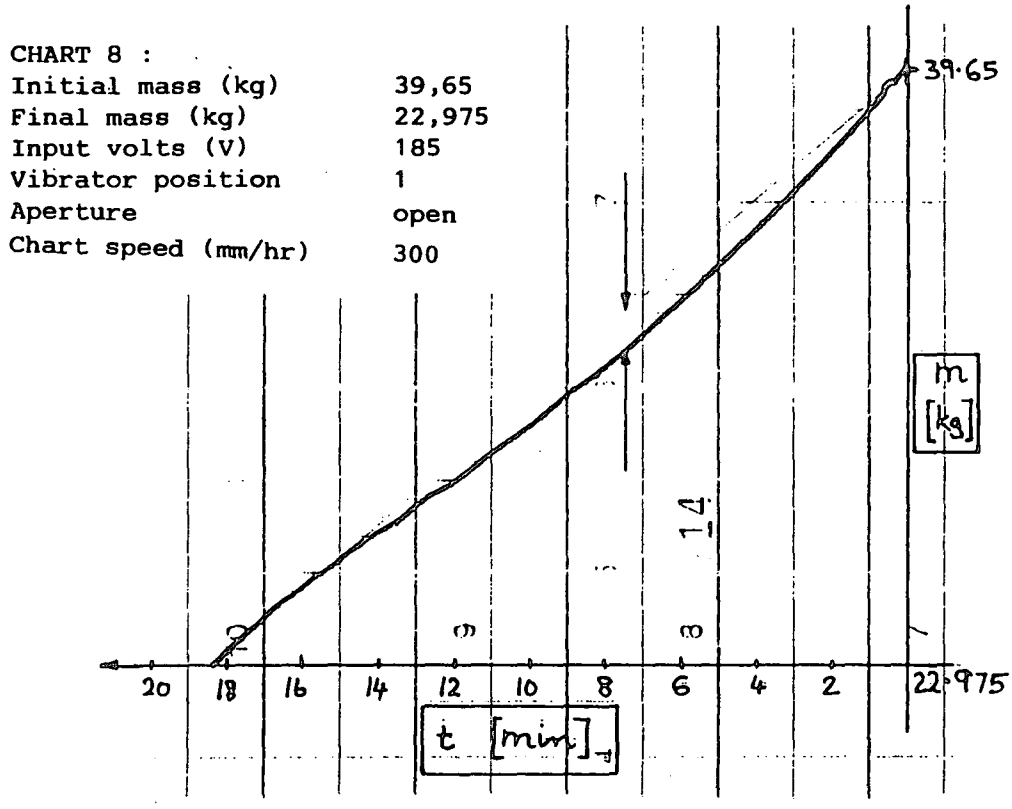

Chart 8. Vibrator position - 1, aperture - open.

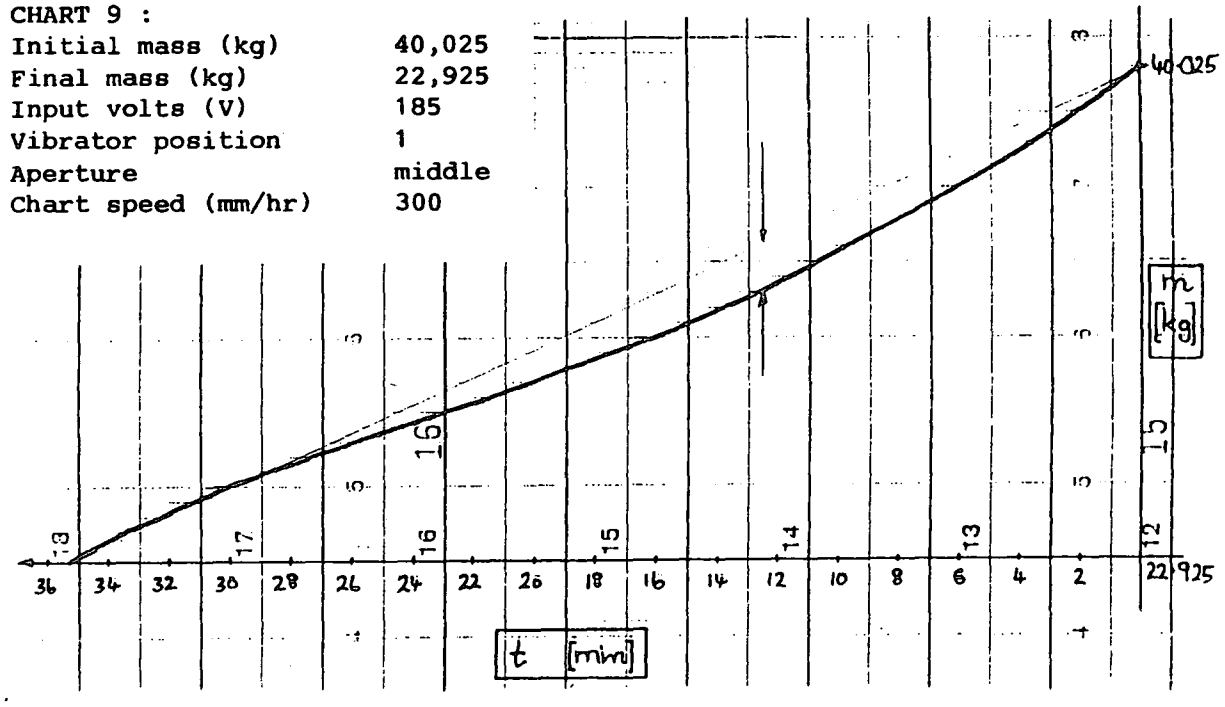

Chart 9. Vibrator position - 1, aperture - middle.

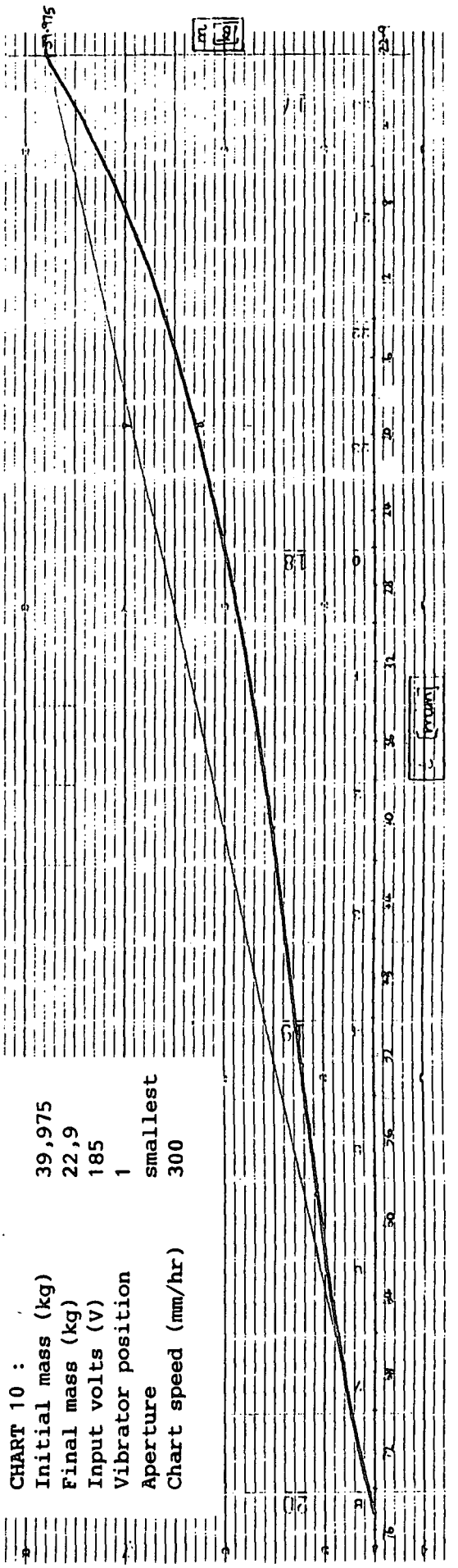

Chart 10. Vibrator position - 1, aperture - smallest.

CHART 11 :

Initial mass (kg)	39,6
Final mass (kg)	22,95
Input volts (V)	185
Vibrator position	2
Aperture	open
Chart speed (mm/hr)	120

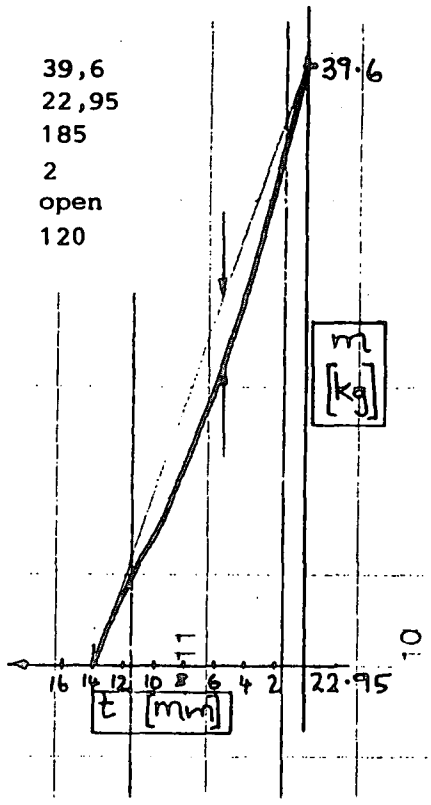

Chart 11. Vibrator position - 2, aperture - open.

CHART 12 :

Initial mass (kg)	39,75
Final mass (kg)	22,975
Input volts (V)	185
Vibrator position	2
Aperture	middle
Chart speed (mm/hr)	120

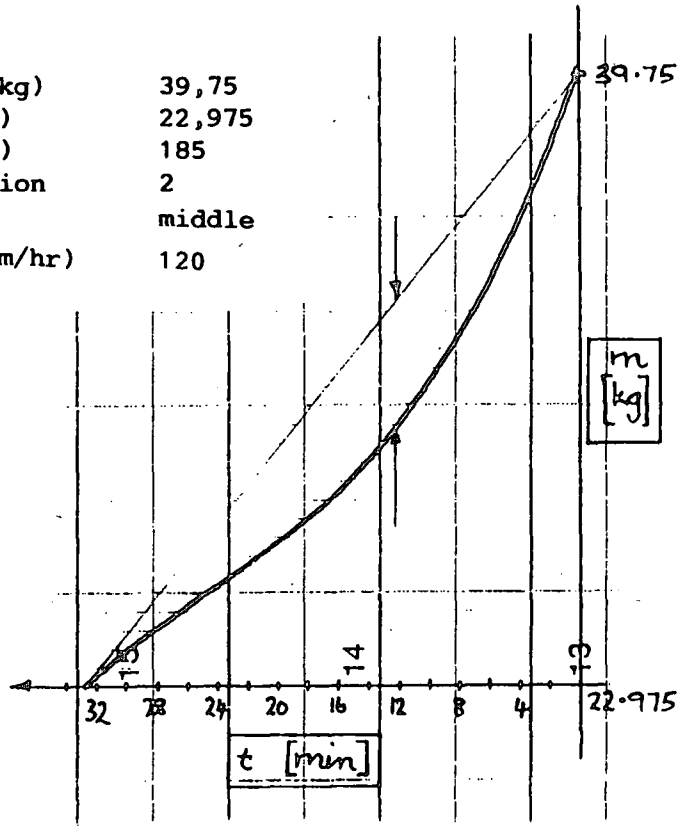

Chart 12. Vibrator position - 2, aperture - middle.

CHART 13 :

Initial mass (kg)	39,65
Final mass (kg)	22,925
Input volts (V)	185
Vibrator position	2
Aperture	smallest
Chart speed (mm/hr)	120

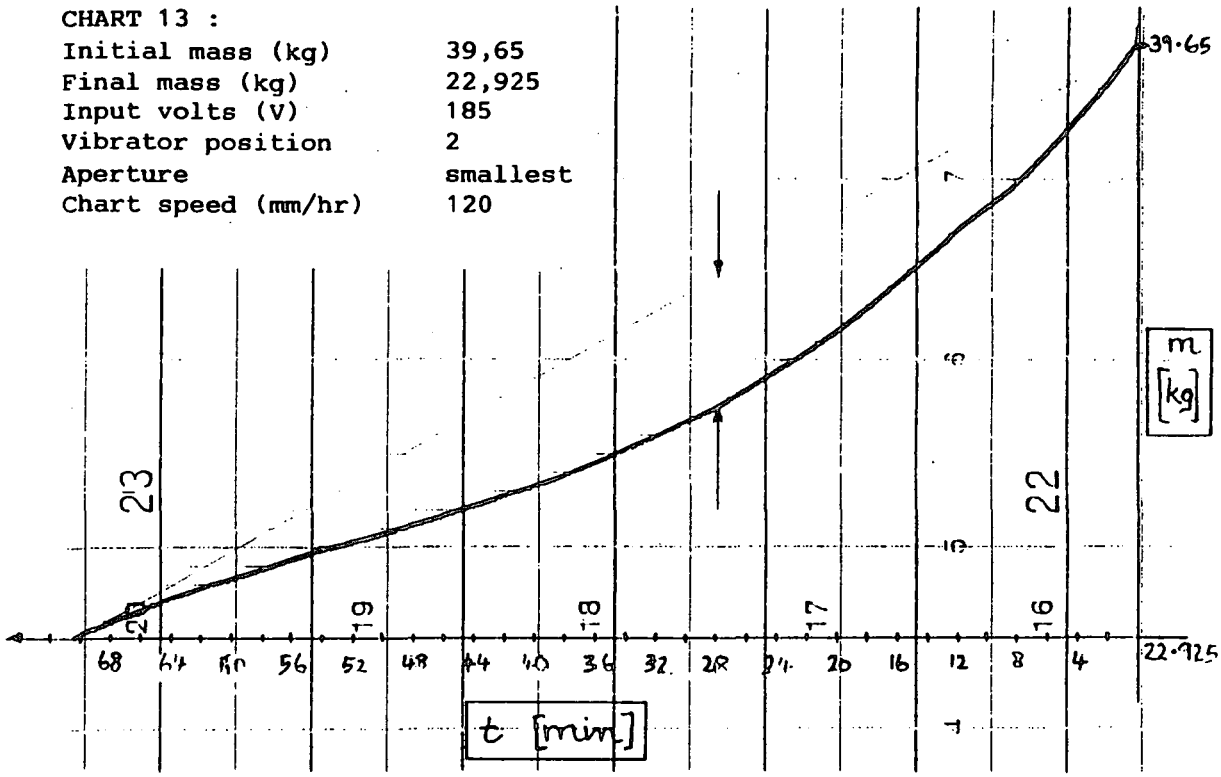

Chart 13. Vibrator position - 2, aperture - smallest.

CHART 14 :

Initial mass (kg)	39,275
Final mass (kg)	22,875
Input volts (V)	185
Vibrator position	3
Aperture	open
Chart speed (mm/hr)	120

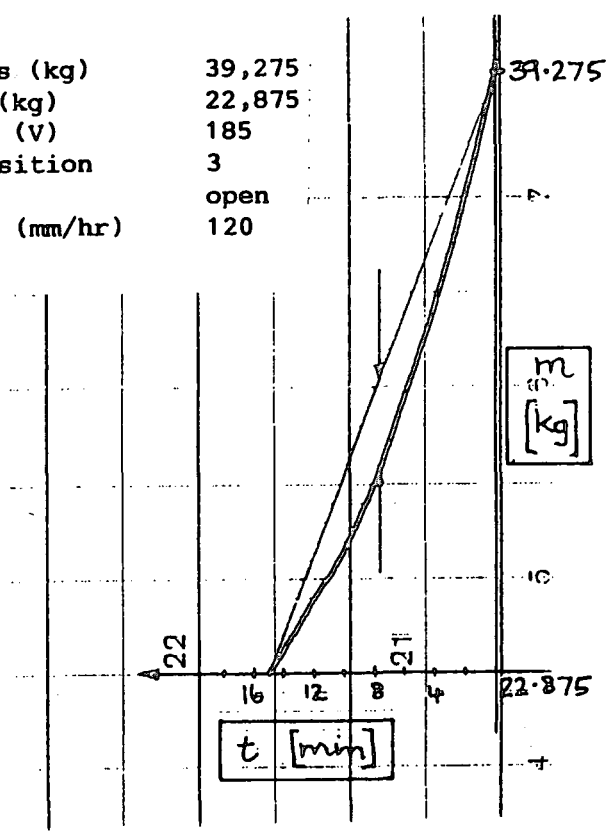

Chart 14. Vibrator position - 3, aperture - open.

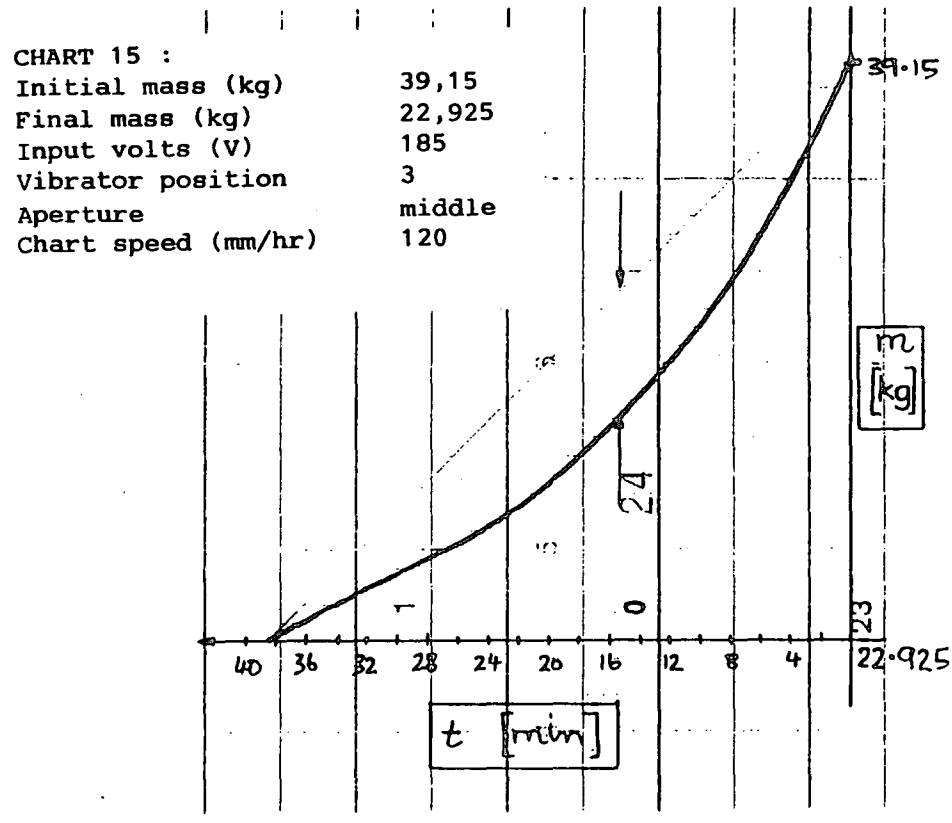

Chart 15. Vibrator position - 3, aperture - middle.

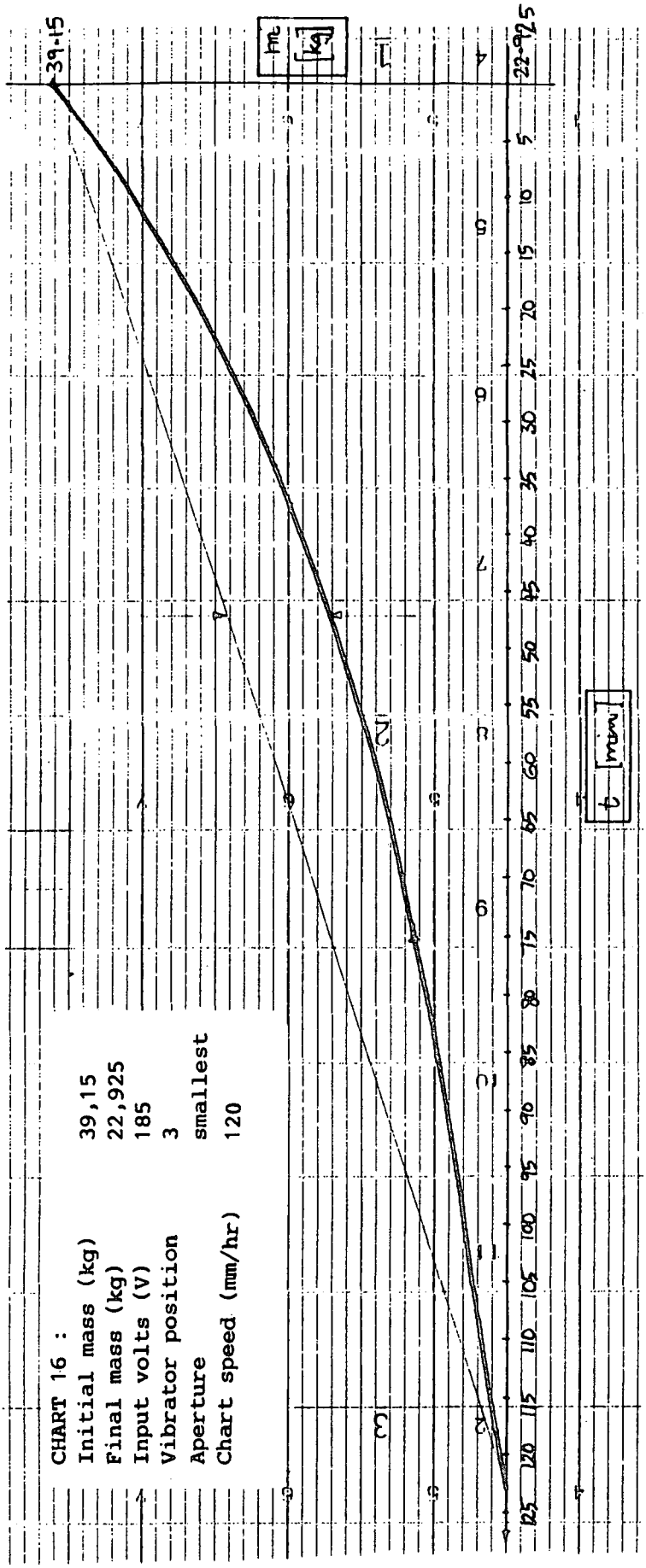

Chart 16. Vibrator position - 3, aperture - smallest.

CHART 17 :	
Initial mass (kg)	38,975
Final mass (kg)	22,975
Input volts (V)	185
Vibrator position	4
Aperture	open
Chart speed (mm/hr)	120

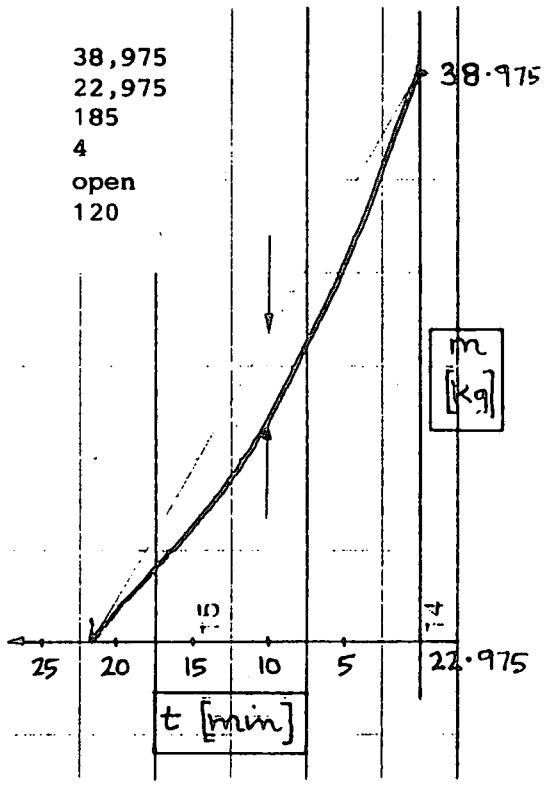

Chart 17. Vibrator position - 4, aperture - open.

CHART 18 :	
Initial mass (kg)	38,625
Final mass (kg)	22,975
Input volts (V)	185
Vibrator position	4
Aperture	middle
Chart speed (mm/hr)	120

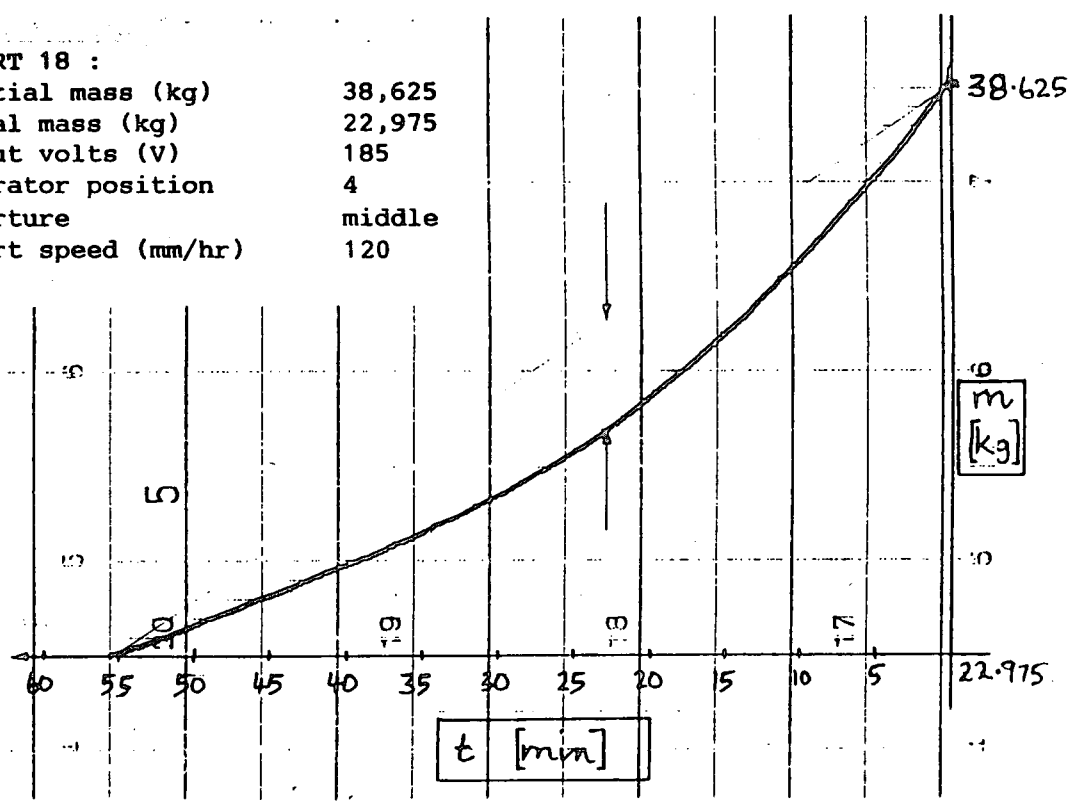

Chart 18. Vibrator position - 4, aperture - middle.

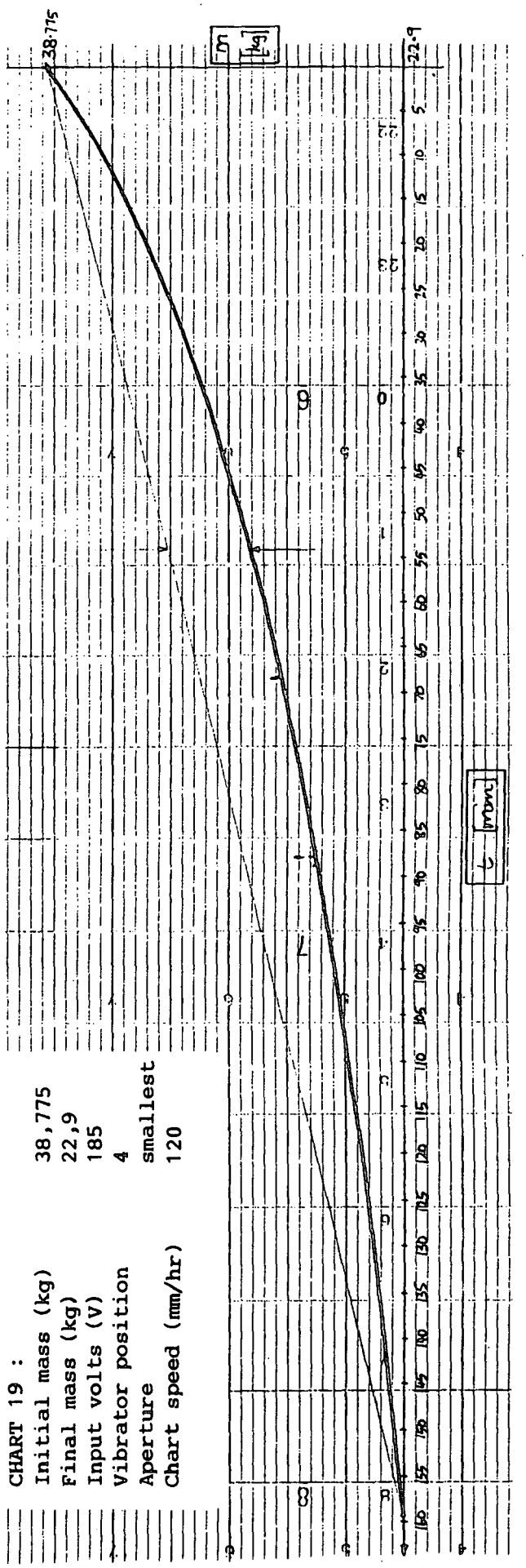

Chart 19. Vibrator position - 4, aperture - smallest.

Appendix B

PROGRAM LISTING

The following program is written in Turbo-Pascal and no claim that it is optimal is made. All comments are written in the braces and these are right justified.

```
program GAINCOMP;

uses dos, CRT;

const

wlen        = 50;          {Sets number of mass values for averaging}
uptime      = 10;          {Sets the loop update time (uptime/10 secs}
stddelay    = 10;          {Time delay between samples - 100ths of sec}
ullim       = 0;                                  {Lower limit of integrator}
uulim       = 150/3600;                           {Upper limit of integrator}

var
     ma, ua, mb, u, ee, ff      : real;
     I, count, CC               : Integer;
     lst, td                    : text;
     fn                         : string[50];
     diff                       : word;
     IP                         : array[1..wlen] of integer;

procedure SETPOINT;                                {Inputs a setpoint}

const
     adcard = 632;

var
     m, G, mave, KK             : Real;
     T1, T2, Y                  : Longint;
     CMD                        : Boolean;
     ANS                        : Char;
     K, BB, F                   : Integer;
     hour, min, sec, sec100     : Word;

procedure READMASS;                        {Inputs mass and converts to kg}

var
     A, B, C                    : real;
     E, J                       : integer;

begin
     port[adcard+3]:=0;              {This section does the A/D conversion}
     port[adcard+0]:=0;                {and converts the mass into a 12 bit}
```

```
      for E:=1 to 7 do                                          {number F}
      A:=port[adcard+4];
      for E:=1 to 7 do
      A:=port[adcard+5];
      B:=port[adcard+1];
      C:=port[adcard+2];
      F:=round((C-16*(int(C/16)))*256+B);
      for I:=wlen downto 2 do                    {This is the start of the digital}
      IP[I]:=IP[I-1];                          {filter, which finds the average of}
      IP[1]:=F;                                  {wlen mass values and gives the}
      m:=0;                                    {answer as mave. This value is then}
      for I:= 1 to wlen do                       {converted to a mass value in kg}
      m:= m+IP[I];
      m:= m/wlen;
      mave:=((((m)-895)/753)*18.2)+11.75;
end;

procedure DIFFER;                          {This procedure is the differentiator}
                                                        {which yields a feedrate}
begin
      ma:=mave;
      ff:=(ma-mb)/(uptime/10);
      mb:=ma;
end;

procedure COMP;                            {This procedure is a comparator or}
                                                          {summing junction}
begin
      ee:=KK-ff;
end;

procedure CONT;                              {This procedure is the controller}
                                                        {which is an integrator}
begin
      u:=(-0.1*ee*uptime/10)+ua;
      if u<ullim then u:=ullim
      else if u>uulim then u:=uulim;
      ua:=u
end;

procedure SETGAIN;                           {This procedure performs gain the}
                                             {scheduling which adjusts the gain}
begin                                      {according to the value of the mass}
      if mave>=21
      then G:=(1000*(exp(ln(10)*(-0.23333*mave+8.4)/20))) else
      if (mave>=18.7) and (mave<21)
      then G:=(1000*(exp(ln(10)*(0.652*mave-10.196)/20))) else
      if (mave>=14) and (mave<18.7)
      then G:=(1000*(exp(ln(10)*(1.4894*mave-25.85)/20))) else
      if (mave<14) and (mave>=13.2)
      then G:=(1000*(exp(ln(10)*(-5)/20))) else
      if mave<13.2
      then G:=(1000*(exp(ln(10)*(-1.5625*mave+15.625)/20)));
      if mave<17
```

```
        then G:=G*(1.909090909-(0.0181818*K));          {This is the second}
end;                                                    {level of gain scheduling}
                                                        {according to the input signal}
procedure OUTPLANT;                                     {This procedure converts the output}
                                                        {to a 12 bit number for conversion}
begin                                                   {via the D/A converter}
        Y:=round(u*G*97.45);                            {to drive the plant}
        if Y<0 then Y:=0;                               {97.45 is a conversion factor}
        if Y>4050 then Y:=4050;
        port[adcard+6]:=(Y and $00FF);
        port[adcard+7]:=((Y and $0F00) shr 8);
end;

begin                                                   {This is the first procedure}
        clrscr;                                         {after the main program}
        writeln('Enter the setpoint between 1 and 50 kg/hr');
        readln(K);
        clrscr;
        KK:=-(K/3600);                                  {Converts setpoint to kg/sec}
        gotoxy(1,24);
        writeln('Press "S" to change setpoint');
        repeat
                gettime(hour,min,sec,sec100);           {Reads real time clock}
                T1:=(hour)*360000+(min)*6000+(sec)*100+(sec100);
                READMASS;
                gotoxy(50,12);                          {This section displays}
                write('mave =  ',mave:10:2,' kg');      {the data on the screen}
                gotoxy(50,14);
                write('sp   =  ',-K:10,' kg/hr');
                gotoxy(50,16);
                write('ff   =  ',ff*3600:10:2,' kg/hr');
                gotoxy(50,18);
                write('ee   =  ',ee*3600:10:2,' kg/hr');
                gotoxy(50,20);
                write('u    =  ',u*3600:10:2);
                gotoxy(50,22);
                write('G    =  ',G:10:2);
                gotoxy(50,24);
                write('Y    =  ',Y:10,' dec');
                gettime(hour,min,sec,sec100);           {Reads real time clock}
                T2:=(hour)*360000+(min)*6000+(sec)*100+(sec100);
                diff:=(T2-T1);                          {Measures time of calculation}
                if (diff) < (stddelay) then
                delay(((stddelay) - (diff))*10);        {Sets delay to stddelay}
                inc(CC);
                if CC = uptime then     {Sets loop updating time in secs [CC/10]}
                begin
                        writeln(td,mave:8:2);           {Writes mave into td for storage}
                        DIFFER;                         {Goes to and executes each of}
                        COMP;                           {these procedures in turn}
                        CONT;
                        SETGAIN;
                        OUTPLANT;
                        CC:=0;
```

```
            end;
            if keypressed then Ans:= readkey;
        until Upcase(Ans)='S';
end;

begin                                          {The main program begins here}
        fn:= 'C:\GARY\prefil.DAT';             {This is where data is written to}
        assign(td,fn);                                        {Puts td into fn}
        rewrite(td);
        for count:=1 to wlen do                {This section zeros all these registers}
        IP[count]:=0;
        CC:=0;
        ee:=0;
        mb:=0;
        ua:=0;
        ff:=0;
        u:=0;
        diff:=0;
        I:=1;
        while I<>2 do
        begin
            clrscr;
            gotoxy(10,18);
            write('1. Input a setpoint');
            gotoxy(10,20);
            write('2. Return to DOS');
            gotoxy(10,23);
            write('Your choice please ?');
            readln(I);
            if I=1 then SETPOINT;
        end;
        close(td);                                        {Closes the data file td}
        clrscr;
end.
```

Appendix C

After the design of the gain scheduling, test runs were done to assess its performance, and these are shown here. These charts revealed that the feedrate was also dependent on the magnitude of the setpoint (as well as the mass remaining in the hopper). First, test runs with the gain scheduling were done, from full to empty, at four different feedrates. These are shown in charts 1 to 4 and the over compensation of the gain is clear in charts 3 and 4. It was then decided to use a second level of compensation (see page 29), and in order to establish the values to be used two feedrates were chosen, 39 kg/hr and 28 kg/hr. The hopper system would be run with only a small amount of raw material and charts 5 and 6 show the results with various modified gain values, as indicated. Finally charts 7 and 8 show complete test runs for these two feedrates with the modified gain as selected on page 30.

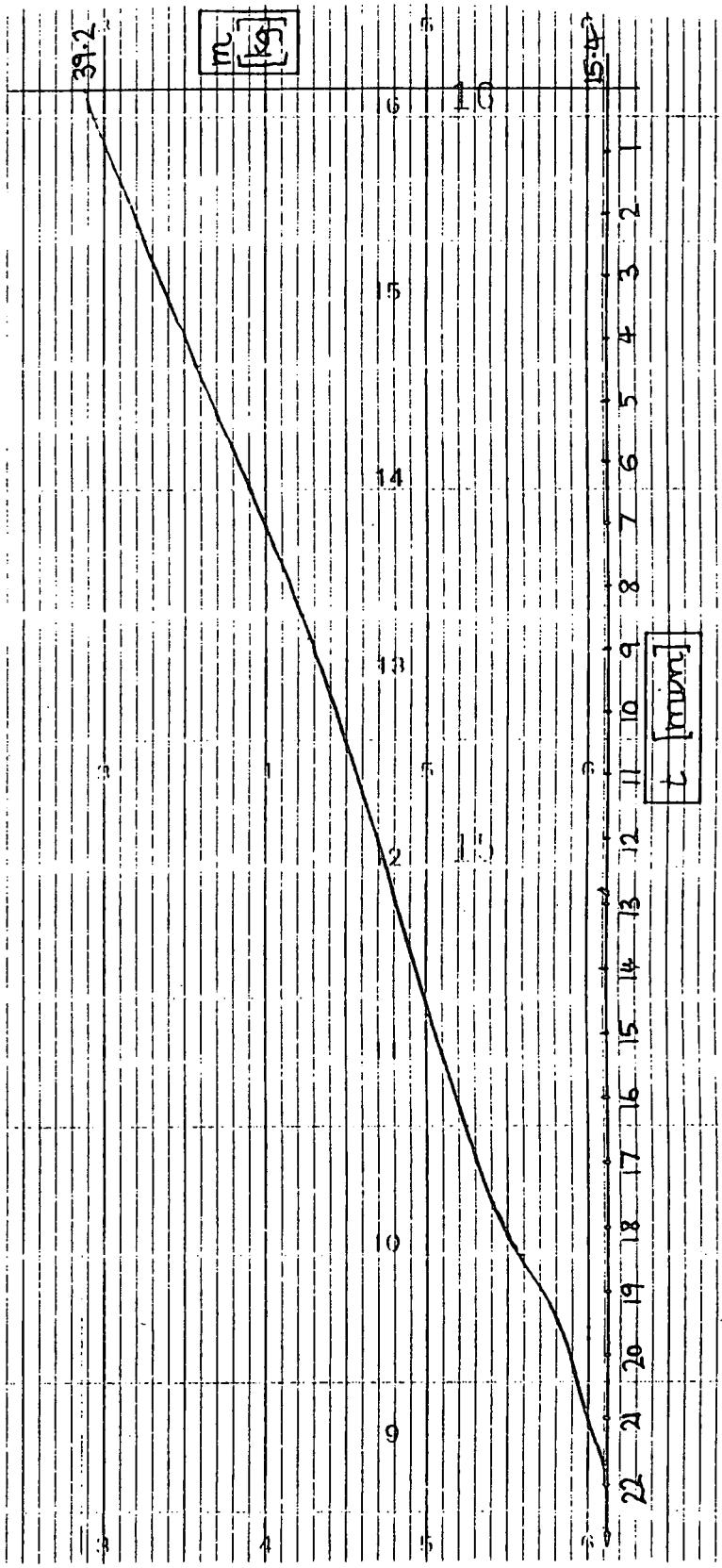

Chart 1. Mass change with gain scheduling, 50 kg/hr.

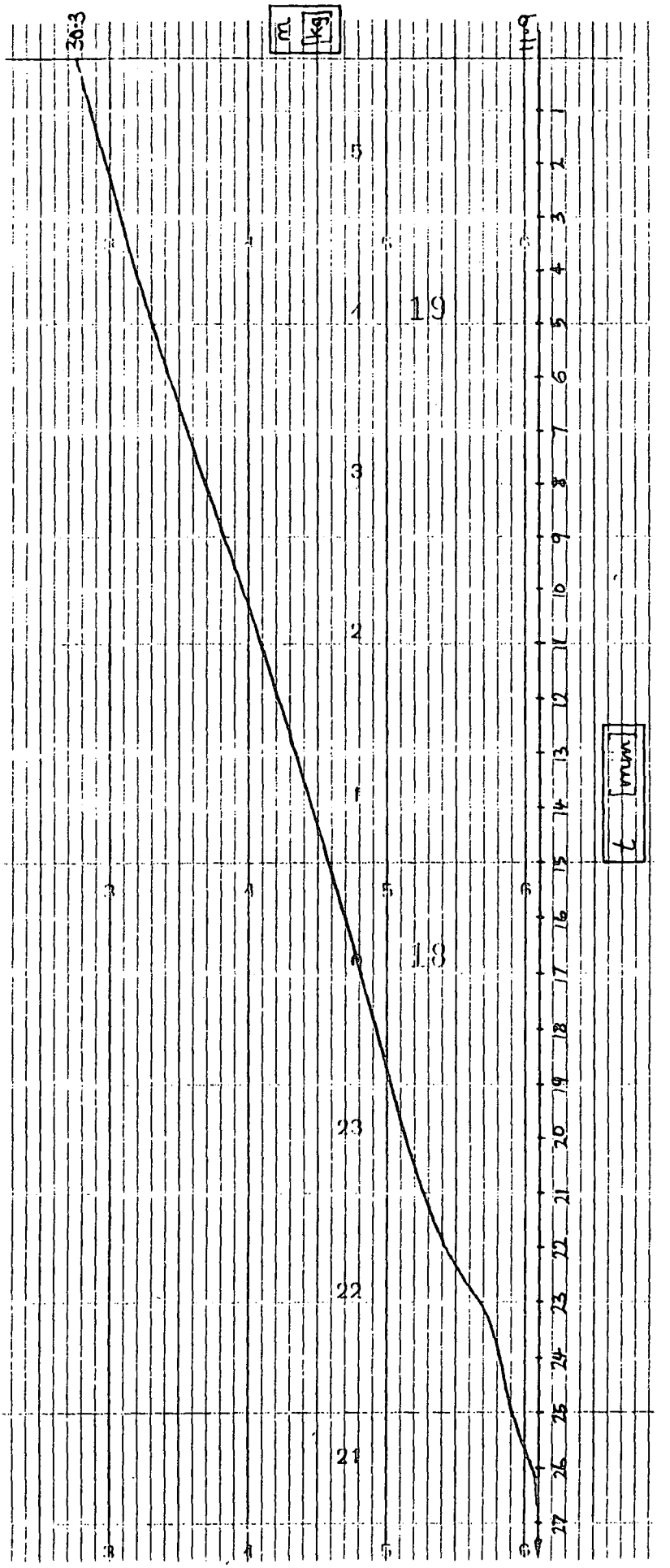

Chart 2. Mass change with gain scheduling, 45 kg/hr.

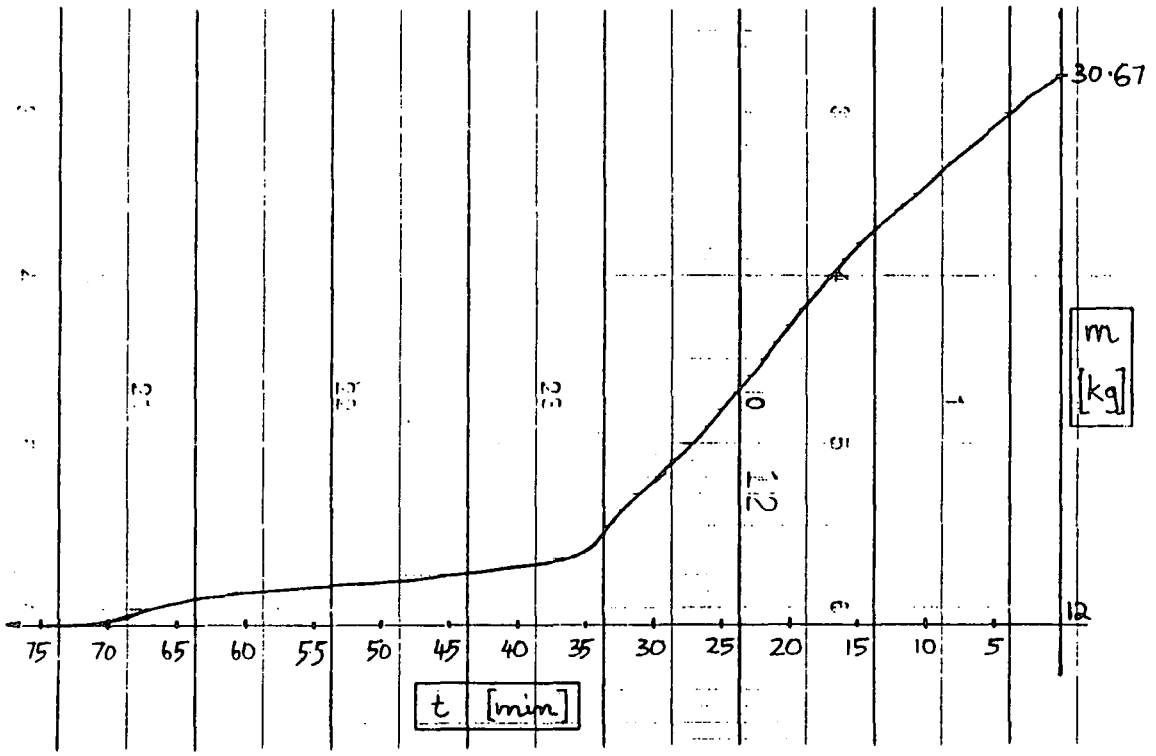

Chart 3. Mass change with gain scheduling, 39 kg/hr.

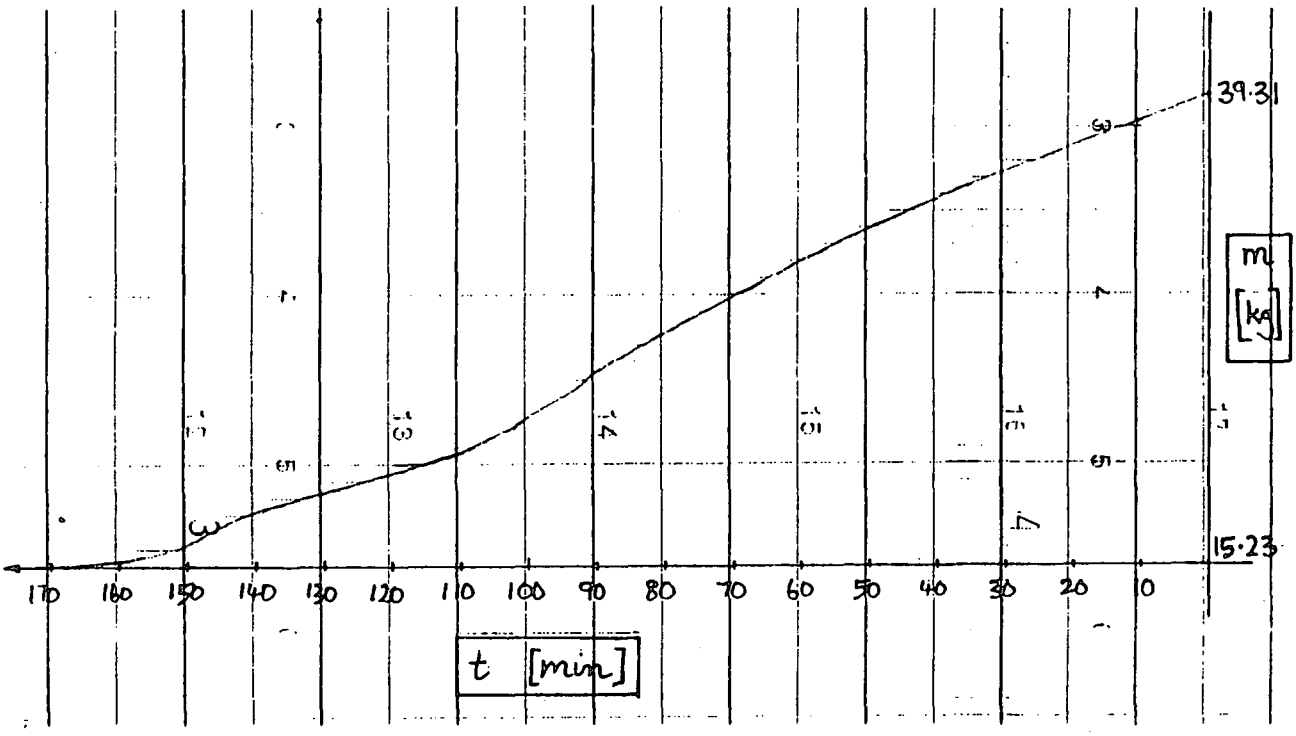

Chart 4. Mass change with gain scheduling, 28 kg/hr.

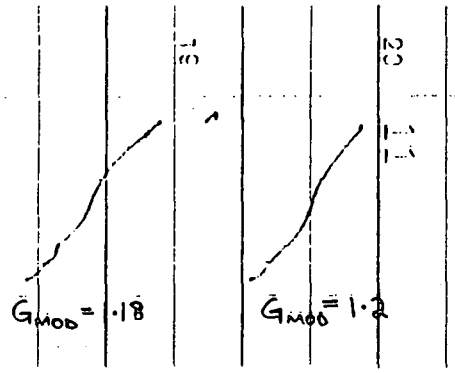

Chart 5. Response near empty with modified gain, 39 kg/hr.

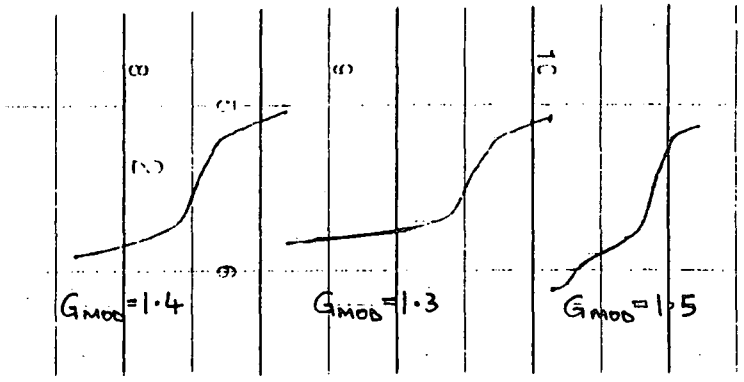

Chart 6. Response near empty with modified gain, 28 kg/hr.

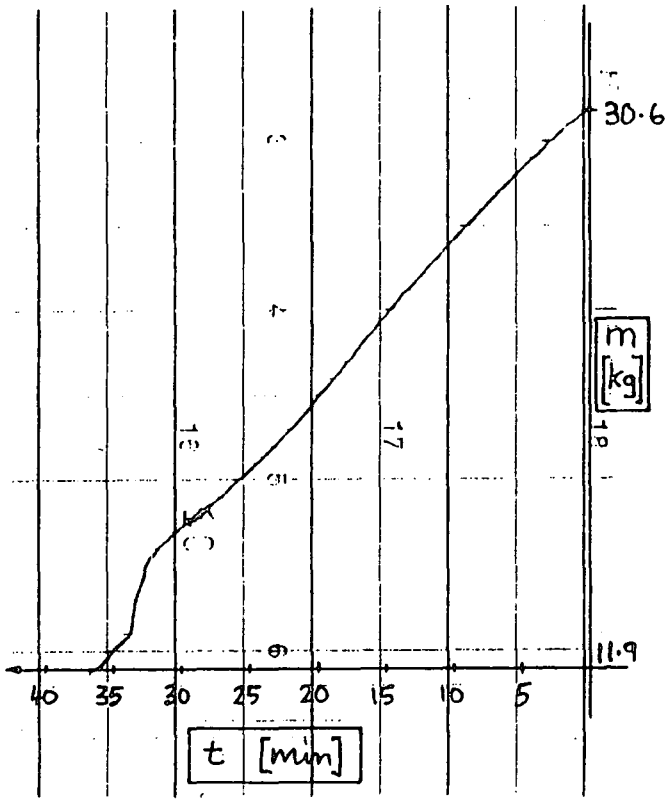

Chart 7. Mass change with final modified gain, 39 kg/hr.

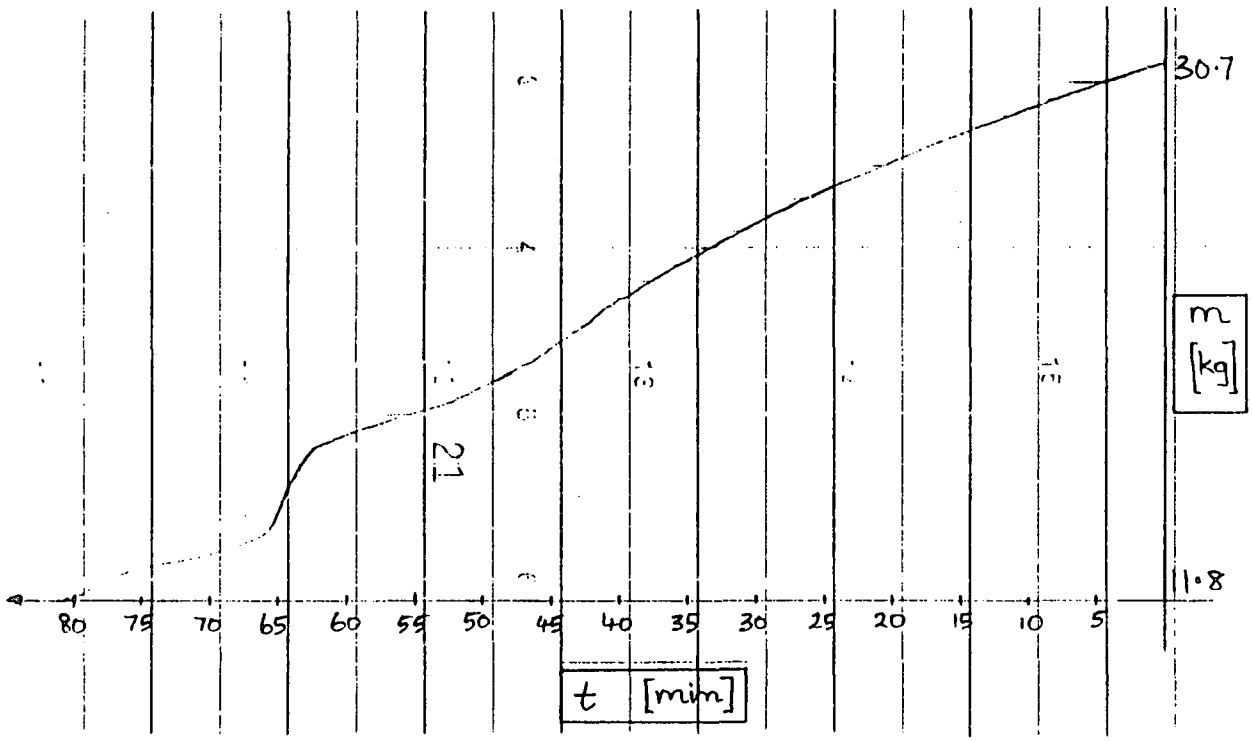

Chart 8. Mass change with final modified gain, 28 kg/hr.